INHIBITED SPONTANEOUS EMISSION OF PERYLENE DYE MOLECULES EMBEDDED IN NANO-CAVITIES

by
Ahmet Akın Ünal

Submitted to the Graduate School of Engineering and Natural Sciences
in partial fulfillment of
the requirements for the degree of
Master of Science

Sabancı University
July 2005

INHIBITED SPONTANEOUS EMISSION OF PERYLENE DYE MOLECULES EMBEDDED IN NANO-CAVITIES

APPROVED BY:

Prof. Dr. M. Naci İnci .....
(Thesis Supervisor)

Prof. Dr. Yani Skarlatos .....

Assist. Prof. Dr. İsmet İnönü Kaya .....

DATE OF APPROVAL: July 29, 2005

Annem, babam ve canım kardeşime ...

ACKNOWLEDGEMENTS

I would like to express my deepest gratitude to my thesis supervisor, Prof. Dr. M. Naci İnci for his continuous guidance and generous supports throughout my study. It was a great pleasure for me to conduct this thesis under his supervision. I am also very grateful to Assist. Prof. Dr. Alper Kiraz from Koç University, who has conducted all of his invaluable experiences about the optical setup and instruments I have used during my studies.

I would like to thank Prof. Dr. Yani Skarlatos and Assist. Prof. Dr. İsmet İnönü Kaya for reading my thesis and offering valuable suggestions.

I would especially like to thank Atilla Özgür Çakmak, İbrahim İnanç and Serkan Baş for always being with me and for all their very helpful comments and advices about my experiments.

I would gratefully acknowledge Eren Şimşek for preparing all of the polymer nanofibers. I would also like to thank Çınar Öncel for giving his valuable time to take the SEM photographs of my samples.

I also want to acknowledge my housemate Özgür Taşdizen for all his supports and generous helps during my studies and Can Sümer for his friendships for the past two years.

I would like to thank Microelectronics and Materials Engineering faculties, staff and students of Sabancı University for providing me with professional experiences.

Finally, I am grateful to my family and Gamze Bakkalcı for their endless encouragements and abundant love during my studies.

ABSTRACT

The radiative properties of molecules placed in cavities differ fundamentally from the radiative properties in free space. Fluorescence lifetime measurements of perylene dye molecules in polymer nanocavities are experimentally studied using time-correlated single photon counting techniques. The fluorescence lifetime of perylene is measured to be 4.8 ns. Perylene is embedded into polyacrylonitrile nanofibers and polymethylmethacrylate films. Spontaneous emission rate of perylene is inhibited by a factor of up to 2.6. Thus, the enhancement of fluorescence lifetime of perylene from 4.8 ns to 12.36 ns for polyacrylonitrile nanofibers and to 12.3 ns for polymethylmethacrylate films is observed.

ÖZET

Oyuklar içerisine yerleştirilmiş moleküllerin ışıma özellikleri ile serbest uzaydaki ışıma özellikleri arasında temel farklılıklar vardır. Zaman korelasyonlu tek foton sayma teknikleri kullanılarak polimer nano-oyukların içerisine yerleştirilmiş perylene boya moleküllerinin ışıma ömürleri deneysel olarak çalışıldı. Perylene'in ışıma ömrü 4.8 ns olarak ölçüldü. Perylene, polyacrylonitrile nanofiberler ve polymethylmethacrylate filmlerin içine yerleştirildi. Perylene'in spontane ışıma oranı 2.6 kata kadar yavaşlatıldı. Dolayısıyla perylene'in ışıma ömrü polyacrylonitrile nanofiberlerde 4.8 ns'den 12.36 ns'ye ve polymethylmethacrylate filmlerde 4.8 ns'den 12.3 ns'ye uzadığı görüldü.

TABLE OF CONTENTS

LIST OF FIGURES

LIST OF ABBREVIATIONS

ADC	Analog to Digital Converter
APD	Avalanche Photodiode
MCA	Multichannel Analyzer
NA	Numerical Aperture
PAN	Polyacrylonitrile
PMMA	Polymethylmethacrylate
PMT	Photomultiplier Tube
TAC	Time-to-amplitude Converter
TCSPC	Time-Correlated Single Photon Counting
Ti:Sa	Titanium Doped Sapphire Laser

CHAPTER 1

INTRODUCTION

Spontaneous emission is the process by which matter may lose energy, resulting in the creation of a photon. After Planck [1] expressed the spectral distribution of electromagnetic radiation in the interior of a cavity in thermal equilibrium and found his law for the mean energy density of the radiation, Einstein [2] demonstrated that spontaneous emission must occur if matter and radiation are to achieve thermal equilibrium. Since then it has been believed that excited atoms inevitably radiate [3]. This view, however, overlooks the fact that spontaneous emission is not an intrinsic property of an isolated matter but of a dynamical interaction between matter and the electromagnetic vacuum field [3, 4].

The spontaneous emission rate, the probability of photon emission per unit time, or more familiarly called the Einstein's A_{21} coefficient, is given by Fermi's golden rule. Both Einstein's A_{21} coefficient and Fermi's golden rule will be explained in Chapter 2. The probability of finding an atom still excited at time t is $exp(-A_{21}t)$. Such an exponential decay law describes an irreversible process, which is the most distinctive feature of spontaneous emission. The source of irreversibility is the continuum of field modes resonantly coupled to the atom. The vacuum fields act as a gigantic reservoir in which the atomic excitation decays away [3].

The primal role of vacuum fields is to drive every excited atom to its ground state. If these vacuum states are to be modified, the spontaneous emission rate can be greatly inhibited or enhanced [3]. Vacuum states can be radically altered by placing an atomic excited state in a confined geometry (so-called cavity) and it should be possible to realize experimental conditions in which an atom is effectively decoupled from the vacuum and cannot radiate. An atom surrounded by a cavity forms a coupled quantum system, and the atom's energy levels are inevitably shifted by the cavity [5]. A dipolar

Van der Waals attraction between the atom and the walls of the cavity arise from alterations in the zero-pint energy of the system [6].

Purcell [7], in 1946, showed that the spontaneous emission rate A_{21} for a two-state system is increased if the atom is surrounded by a cavity tuned to the transition frequency, υ. If the quality factor of the cavity is Q, then the spontaneous rate in the cavity is $A_c \approx Q\ A_{21}$. Physically, the cavity enhances the strength of the vacuum fluctuations at υ, increasing the transition rate. Conversely, the decay rate decreases when the cavity is mistuned. If υ lies below the fundamental frequency of the cavity, spontaneous emission is significantly inhibited. This is known as the cavity or Purcell effect [7].

Looking from the wavelength point of view, it can be said that the mode structure of the vacuum field is dramatically altered in a cavity whose size is comparable to the wavelength. It is suppressed (inhibited) if the cavity has characteristic dimensions which are small compared to the radiation wavelength, and enhanced if the cavity is resonant. In the case of an ideal cavity, no mode is available for the photon and spontaneous emission cannot occur [5].

Researches on spontaneous emission rate modifications belong to a new field of atomic physics and quantum optics called Cavity Quantum Electrodynamics [3].

Many experimental and theoretical efforts have addressed the modification of the spontaneous emission process since Purcell's proposal. The pioneering experimental work showing the inhibited spontaneous emission dates back to 1970 when Drexhage [8] demonstrated that the radiative decay rates (fluorescence lifetimes) of a thin dye film placed close to a flat metallic mirror were different from those in free space. The decay time of the emission of radiation (fluorescence, phosphorescence) varies due to the presence of such an interface.

Drexhage investigated this effect on a europium-dibenzoylmethane complex, which is an organic dye. The molecules were placed at a well-defined distance (6770 Å) from a gold mirror. Absorbing the ultraviolet light, Eu^{3+}-ion fluoresces with high quantum yield at about 632 nm. The mirror influences both the angular distribution of the fluorescence intensity and the fluorescence decay time.

Considering a molecule placed in the center of a spherical mirror, Drexhage showed both enhanced and inhibited spontaneous emission just by playing with the radius of the mirror. When the radius of the spherical mirror is adjusted to be 1.75 λ, the probability for radiation per unit time (Einstein's A_{21} coefficient) will be twice as

large as without the mirror. This means the decay time of the molecule in the center of the mirror will be half the decay time of the molecule in free space. As this gives a decrease in the lifetime, there is an enhancement in the spontaneous emission rate. On the other hand, if the radius of the spherical mirror is for instance 2 λ, the excited molecule cannot radiate at all, and it will stay high forever. In this case, there is an infinite decay time.

In the 1980s and 1990s several other groups have demonstrated the possibility of controlling radiative decay rates by putting emitters in confined geometries such as the spaces between two flat substrates or reflectors [9-12], between mirrors of high-finesse optical cavities [11,13], and in whispering gallery mode resonators [14]. Chew analytically calculated that atoms inside sub-wavelength (the transition wavelength is superior to the dimensions of the confining media) spheres exhibit modifications in the spontaneous emission [15]. In a recent paper, the authors showed an inhibiton of the spontaneous emission up to 3 times by using europium ions that are embedded in dielectric nanospheres [4].

Just as the cavity below radiation wavelength suppresses vacuum fluctuations, a resonant cavity enhances them. The first observation of enhanced spontaneous emission has been performed in 1983 by Goy et al [16]. They used the millimeter wave regime for Rydberg atoms of sodium coupled to a Fabry-Perot cavity. The emission rate was enhanced by a factor of approximately 500. Heinzen et al observed enhanced spontaneous emission by employing a spherical Fabry-Perot resonator and enhanced the emission by a factor of 19. Enhanced emission was also observed in whispering-gallery mode resonator [17,18].

These spectroscopic changes can be qualitatively understood by saying that the molecule is “dressed” by the surrounding. In the case of a planar surface, for instance, the lifetime variation of the excited state depends on the distance between the molecule and the surface in a rather complex manner. At very large distances, this variation displays an oscillatory regime due to interference phenomena; whereas in the near zone, the nonradiative energy transfer between the molecule and the surface produces a strong decrease of the lifetime [19].

The aim of this thesis is to propose various polymer cavities as host media for perylene dye molecules, in which the embedded molecules suffer to radiate, thus resulting to an inhibition in the spontaneous emission rate. Inhibiting the spontaneous

emission rate means increasing the decay lifetime (τ_{21}) of the molecule, where $\tau_{21} = (A_{21})^{-1}$. Perylene has a reported lifetime of around 4.5 ns [20-22].

Polyacrylonitrile (PAN) nanofibers and polymethylmethacrylate (PMMA) films were used as cavities, and organic perylene compounds were embedded into these geometries. The reason behind using PAN and PMMA polymers as host media is that they have similar structure with perylene molecules, which is necessary in order to be able to prepare polymer/dye blends by dissolving both perylene and the polymer in the same solvent group. Rigorous stirring during the preparation causes perylene molecules to be embedded and confined into the polymers.

Choosing perylene as the fluorescent molecule has also some important reasons. First of all, perylene has a very good absorption at the excitation wavelength of 400 nm. Secondly, the femtosecond Ti:sapphire laser has a repetition rate of 76 MHz, thus corresponding to a pulse every 13 nanoseconds, which is considered to be enough for up to 2 or 3 times of extension in the perylene lifetime (4.5 ns).

The outline of the thesis is arranged as follows: In chapter 2, theoretical aspects regarding atom-radiation interaction is given. Planck's radiation law is explained in order to deduce Einstein's *A* and *B* coefficients, and the spontaneous emission is then presented in detail. This is followed by the general principles of fluorescence spectra and time-domain lifetime measurements in the third chapter. It forms the basis for time-correlated single photon counting techniques. Chapter 4 describes the experimental methods employed to prepare perylene embedded polymer samples and the optical methods used to measure fluorescence lifetimes. Chapter 5 presents the results on inhibited spontaneous emission of perylene and is followed by the discussion of the found results. The sixth chapter concludes the work of the thesis and presents some future work suggestions.

CHAPTER 2

ATOM - RADIATION INTERACTION

In this chapter, the thermal excitation of electromagnetic radiation and the basic kinds of interactions that can occur between light and atomic transitions, beginning from the theories of Planck and Einstein, will be discussed. These phenomena are closely related, as the absorption and emission of light by atoms provide the mechanisms explaining the amount of excitation of the electromagnetic radiation and the conditions of thermal equilibrium.

2.1. Planck's Radiation Law

The quantum theory of light began in 1900 when Planck [1] postulated that the energy of a harmonic oscillator is quantized by measuring the spectral distribution of the electromagnetic energy radiated by a thermal source. A harmonic oscillator of angular frequency ω can have only energies that are integer multiples of the fundamental quantum $\hbar\omega$, where $\hbar=h/2\pi$ and h is Planck's constant. A radiation field in space is usually described in terms of harmonic oscillators, one for each mode of radiation. The levels of this oscillator correspond to states with 0, 1, 2,…, n photons of energy $\hbar\omega$ [3]. For n=0 the oscillator is in its ground state, but a finite amount of energy $\hbar\omega/2$ is still present in the field. This is the zero-point (vacuum) energy of the oscillator. The n^{th} excited state has n quanta of energy $\hbar\omega$ in addition to the zero-point energy of the oscillator. The zero-point or vacuum energy remains infinite [23].

Planck's law expresses the spectral distribution of electromagnetic radiation in the interior of a cavity in thermal equilibrium, which is called as the black-body radiation [1]. In this section, it is aimed to find Planck's law for the mean energy density of the radiation, which will be frequently used in defining Einstein's coefficients

in Section 2.2. In order to find the mean energy density of radiation, we first have to find the density of modes, then their mean energy at temperature *T*.

The number of modes per unit volume of cavity having wavevectors between *k* and *k*+*dk*, that is, the density of field modes, is:

$$\rho(k)dk = k^2 dk/\pi^2 \tag{2.1.1}$$

Relating the angular frequency ω of a mode to its wavevector by $\omega=ck$, the density $\rho(\omega)d\omega$ of modes in the frequency range ω to $\omega+d\omega$ is found as

$$\rho(\omega)d\omega = \omega^2 d\omega/\pi^2 c^3 \tag{2.1.2}$$

In thermal equilibrium at temperature *T*, the probability *P(n)* that the mode oscillator is thermally excited to its *n*th excited state is given by Boltzmann factor

$$P(n) = \frac{\exp(-E_n/kT)}{\sum_n \exp(-E_n/kT)} \tag{2.1.3}$$

where $E_n = (n+\frac{1}{2})\hbar\omega$ is the discrete energy levels of a quantum harmonic oscillator.

The mean number $\langle n\rangle$ of photons excited in the field mode at temperature *T* is therefore [23]

$$\langle n\rangle = \sum_n nP(n) = \frac{1}{\exp(\hbar\omega/kT)-1} \tag{2.1.4}$$

Multiplying $\langle n\rangle$ with $\hbar\omega$ gives the mean energy of the modes.

Having found the density $\rho(\omega)d\omega$, and the mean energy $\langle n\rangle\hbar\omega$, of the modes, we can now find the mean energy density of the radiation in the modes of frequency ω at temperature *T* as [23]

$$\langle W_T(\omega)\rangle d\omega = \langle n\rangle\hbar\omega\rho(\omega)d\omega = \frac{\hbar\omega^3}{\pi^2 c^3}\frac{d\omega}{\exp(\hbar\omega/kT)-1} \tag{2.1.5}$$

By using this result, the Einstein's coefficients will be defined in the following section.

2.2. Einstein's *A* and *B* Coefficients

The interaction of electromagnetic radiation with atoms was discussed by Einstein [2] in 1917. Einsteins's hypotheses regarding the interactions of radiation with matter have been the basis of Quantum Optics. Einstein postulated three forms of energy exchange: absorption, spontaneous emission, and stimulated emission.

Considering a gas of N identical atoms placed in a cavity, with each atom having a pair of energy levels E_1 and E_2, the energy difference $E_2 - E_1 = \hbar\omega$ is equal to that of a quantum of radiation. Photons of frequency ω are emitted or absorbed by atoms that make transitions between the two states. Suppose that the two atomic levels have degeneracies g_1 and g_2, and the mean numbers of atoms in the two multiplet states are denoted by the level populations N_1 and N_2 , and no atoms are in any other states, so that $N_1+N_2=N$. The levels are illustrated in Fig.1.

The mean energy density of radiation at frequency ω consists of the thermal contribution given by Planck's law and a contribution from external sources of electromagnetic radiation, denoted by a subscript E. Thus the total energy density is:

$$\langle W(\omega)\rangle = \langle W_T(\omega)\rangle + \langle W_E(\omega)\rangle \qquad (2.2.1)$$

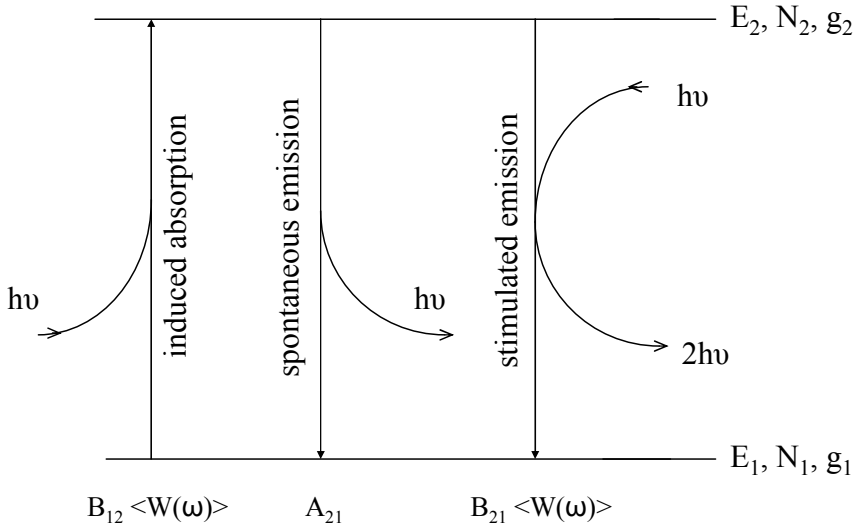

Fig.1. Three forms of energy exchange between matter and radiation, and the transition rates for these processes postulated by Einstein. The excited state can return to the lower state spontaneously as well as by a process stimulated by radiation already present at the transition frequency.

In absorption, as it is seen on Figure 1, a photon transfers its energy to the molecule and induces a transition from level 1 to level 2. In stimulated emission, on the other hand, a photon interacts with a molecule already in level 2 and induces the emission of another photon with a transition down to level 1. Both absorption and stimulated emission require the initial presence of radiation and have rates proportional to the radiation density, $\langle W(\omega)\rangle$ (J.s/m^3), at frequency ω. The rates of absorption and stimulated emission can be expressed as $\langle W(\omega)\rangle B_{12}$ and $\langle W(\omega)\rangle B_{21}$.

A_{21}, B_{12}, and B_{21} are now called the Einstein coefficients for spontaneous emission, absorption, and stimulated emission, respectively. Considering the influences of the transition rates (Einstein coefficients) on the atomic level populations N_1 and N_2, the rates of changes of these populations are given by

$$dN_1/dt = -dN_2/dt = N_2A_{21} - N_1B_{12}\langle W(\omega)\rangle + N_2B_{21}\langle W(\omega)\rangle \tag{2.2.2}$$

The thermal energy density $\langle W_T(\omega)\rangle$ can be written in terms of Einstein coefficients by using a case called steady state, where the population-time derivatives vanish and the above equation reduces to

$$N_2A_{21} - N_1B_{12}\langle W(\omega)\rangle + N_2B_{21}\langle W(\omega)\rangle = 0 \tag{2.2.3}$$

Thus, Planck's thermal energy density is found when we neglect the radiative energy density

$$\langle W_T(\omega)\rangle = \frac{A_{21}}{(N_1/N_2)B_{12} - B_{21}} \tag{2.2.4}$$

The mean numbers of atoms in the two levels in thermal equilibrium are related by Boltzmann's law as

$$\frac{N_1}{N_2} = \frac{g_1\exp(-E_1/kT)}{g_2\exp(-E_2/kT)} = \frac{g_1}{g_2}\exp\left(\frac{\hbar\omega}{kT}\right) \tag{2.2.5}$$

Substituting this result into the equation (2.2.4) for $\langle W_T(\omega)\rangle$ gives

$$\langle W_T(\omega)\rangle = \frac{A_{21}}{(g_1/g_2)\exp(\hbar\omega/kT)B_{12} - B_{21}} \tag{2.2.6}$$

Equation (2.2.6) gives the thermally excited radiative energy density, which is found from the definitions of the Einstein coefficients, must be consistent with Planck's law for the same physical quantity, given by equation (2.1.5). The two expressions are identical at all temperatures T only if

$$g_1B_{12} = g_2B_{21} \tag{2.2.7}$$

As a result, the coefficient of spontaneous emission can be easily interrelated to the coefficients of stimulated emission or absorption [2] by equating equations (2.1.5) and (2.2.6) under the condition given in equation (2.2.7):

$$(\hbar\omega^3/\pi^2c^3)B_{21} = A_{21} \tag{2.2.8}$$

2.3. Spontaneous Emission

In spontaneous emission, a molecule in the excited state can emit a quantum of radiation and undergo a transition down from energy level 2 to level 1 (see Fig.1). This process can be understood as resulting from the coupling of the atomic electron to the electromagnetic field in its vacuum state.

If the radiation is at or near visible wavelengths, spontaneous emission is commonly called luminescence. Further, if both states have the same multiplicity (in terms of electronic spin; usually both singlet states), then it is called fluorescence, of which detailed information is present in Chapter 3.

Spontaneous emission does not have the directional properties of stimulated emission. As the light produced by spontaneous emission is completely independent of the incident beam, it can excite any mode of the cavity that satisfies energy conservation. Thus the propagation direction, polarization and phase of the spontaneously emitted light are arbitrary [23]. After the absorption process, the excited atoms eventually return to their lower states either by stimulated or by spontaneous emission. The fraction of the spontaneous emission rate to the total emission is found by using equation (2.2.8) as

$$\frac{A_{21}}{A_{21} + B_{21}\langle W \rangle} = \frac{1}{1 + \left(\langle W \rangle / W_s\right)} \tag{2.3.1}$$

where $W_s = \hbar\omega^3 / \pi^2 c^3$ is defined as the saturation radiative energy density. This fraction of the absorbed energy is re-emitted in random directions, while only a small part being in the same mode as the incident beam.

On the other hand, if the incident beam is removed from the equation (2.2.2), and its energy density is set equal to zero, the rate equation reduces to

$$\frac{dN_2}{dt} = -A_{21} N_2 \tag{2.3.2}$$

The rate of emission is thus proportional to the number of atoms in the excited state, N_2. The above equation can be solved to give

$$N_2(t) = N_2(0) \exp(-t/\tau_{21}) \tag{2.3.3}$$

where $N_2(0)$ is the initial number of atoms in the excited state, and τ_{21} is the lifetime of the transition, $\tau_{21} = (A_{21})^{-1}$ [23]. Every decaying atom emits a quantum $\hbar\omega$, and the emitted light intensity falls off with the same exponential time dependence.

Observation of this fluorescent emission is an experimental means of measuring the Einstein's A_{21} coefficient.

The rate A_{21} for spontaneous transitions from initial state $|i\rangle$ to final state $|f\rangle$ can be written by Fermi's Golden Rule, which is a way to calculate the transition rate between two states of a system using perturbation theory, which means that it is an approximation. The transition probability per unit of time is given by [23]

$$A_{21} = \frac{1}{\tau} = \frac{2\pi}{\hbar^2} \sum_f \left| \langle f | \hat{H}_{ED} | i \rangle \right|^2 \delta(\omega_f - \omega_i) \tag{2.3.4}$$

Here $|i\rangle$ is the excited state of the atom in the absence of any photons, $|f\rangle$ is the final state of the atom with a single photon. H_{ED} is the interaction Hamiltonian for the atom-field interaction ($H_{ED} = e\ D.E_0\ cos(\omega t)$), where the main contribution to it arises from the potential energy of the electric dipole in the electric field of the light beam. Finally, $\delta(\omega_f - \omega_i)$ is the Dirac delta-function, which is introduced in the excitation probability function.

The radiative lifetime of an excited atom is found either by relating it to Einstein's B_{21} coefficient or by using quantized interaction Hamiltonian, of which the derivations will not follow here. The total spontaneous emission rate is obtained by summation of the spontaneous contribution over all modes, and the radiative lifetime is given by

$$A_{21} = \frac{1}{\tau} = \frac{e^2 \omega_0^3 g_1 D_{12}^2}{3\pi\varepsilon_0 \hbar c^3 g_2} \tag{2.3.5}$$

D_{12} is known as the transition dipole moment, c is the speed of light and e is the electron charge.

CHAPTER 3

FLUORESCENCE SPECTROSCOPY AND LIFETIME MEASUREMENTS

3.1. Electronic Transitions

Luminescence is the emission of light from any substance and occurs from electronically excited states. Actually it is a special name for spontaneous emission occurring at or near visible wavelengths. Luminescence is divided into two categories: fluorescence and phosphorescence, depending on the nature of the excited state [24]. In fluorescence, the radiation is emitted during a transition between electronic states of the same multiplicity (electronic spin); that is, between singlet states. However, in phosphorescence the radiation is emitted between electronic states of different multiplicities, for example between a triplet and a singlet state [25].

Electron spin is described by a spin quantum number, s (the analogue of l for orbital angular momentum quantum number), with s=1/2. The spin can be clockwise or counterclockwise, which are distinguished by the spin magnetic quantum number, m_s, which can only take values +1/2 or -1/2 (m_s=±s). An electron with m_s=+1/2 is denoted as a spin up (↑), and an electron with m_s=-1/2 is denoted as a spin down (↓) electron [26].

An ordinary spin-paired (antiparallel) state (↑↓) is called a singlet state. Two spin momenta cancel each other and there is no net spin in a singlet state (S=0 and M_s=0). S is the total spin angular momentum quantum number, and the value of S is called the multiplicity. S takes only the values 1 and 0. The higher the multiplicity, the more electrons there are in the atom spinning in the same direction. The spin angular momenta of two parallel spins add together to give a nonzero total spin, and the resulting state is called a triplet state (S=1 *and* M_s=+1, 0, -1) [26]. The names singlet and triplet come from the concept that there are three ways of achieving a nonzero total

spin (triplet), but only one way to achieve a zero spin (singlet). Figure 1 shows an arrangement of singlet and triplet states together with the non-radiative (wavy arrows) and radiative (straight arrows) decay processes following an induced absorption.

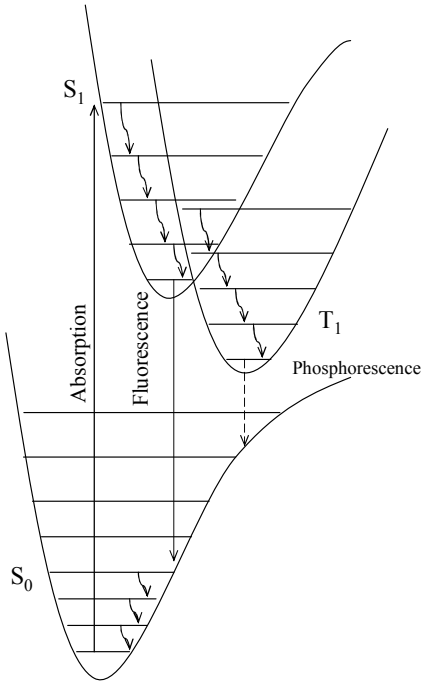

Fig.1. Absorption, fluorescence and phosphorescence by a diatomic molecule [25]. S_0 is the ground singlet state, S_1 is the excited singlet state and T_1 is the triplet state. Wavy arrows represent radiationless decays.

The processes which occur between the absorption and emission of light are usually illustrated by a Jablonski diagram [27].

3.1.1. Jablonski Diagram

A typical Jablonski diagram is shown in Figure 2. The singlet ground, first, and second electronic states are depicted by S_0, S_1, and S_2, respectively, and the triplet state is labeled as T_1 [24]. The transitions between states are shown as vertical lines to illustrate the instantaneous nature of light absorption.

Following light absorption, several processes usually occur. The molecule can chemically react or the molecule can lose its energy in a collision with another molecule, and it may make a transition to another excited electronic state. Such a non-radiative transition from one singlet state to another singlet state, between states of the same multiplicity, is called *internal conversion*, and generally occurs in 10^{-12} s or less.

Since fluorescence lifetimes are typically near 10^{-8} s, internal conversion is generally complete prior to emission [25].

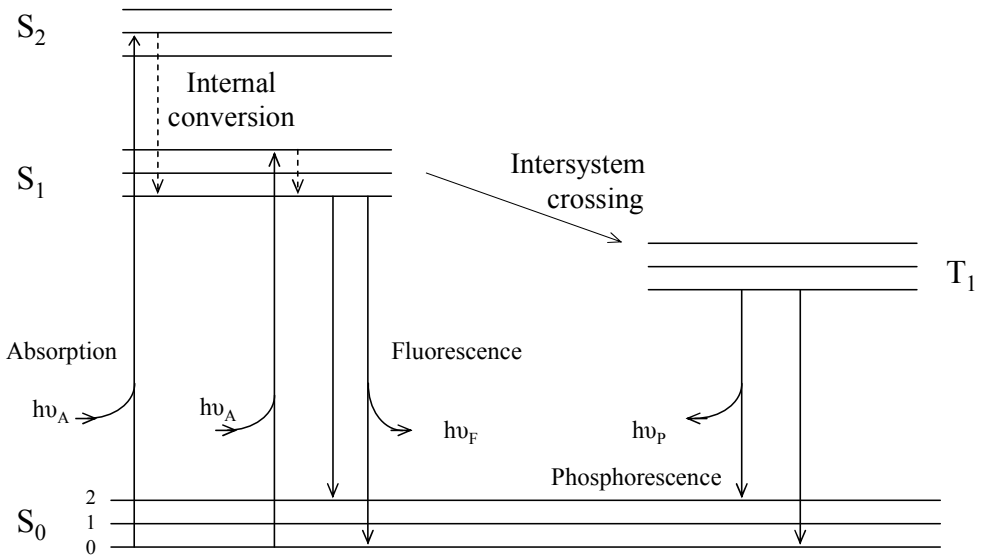

Fig.2. One form of a Jablonski diagram [24].
The energy $h\upsilon_A$ is greater than $h\upsilon_F$, and $h\upsilon_F$ is greater than $h\upsilon_P$.

Hence, fluorescence emission results from a thermally equilibrated excited state, that is, the lowest energy vibrational state of S_1. Some kind of non-radiative transitions between states of different multiplicities are also possible and they are called *intersystem crossing* [25]. The examination of the Jablonski diagram also reveals that the energy of the emission (fluorescence and phosphorescence) is typically less than that of the absorption.

3.1.2. Fluorescence

As it was briefly stated, when a ground state (S_0) molecule is excited to the first excited singlet state (S_1), collisions with other molecules can remove vibrational energy from the excited molecule in a process called vibrational relaxation. In addition to the vibrational relaxation, other non-radiative decay processes, such as rotation and translation of the surrounding molecules also convert the excitation energy into thermal motion of the environment [26]. Figure 1 shows these relaxation processes with wavy lines. Thus, the excited molecule ends up in the lowest vibrational state of S_1. When the excited molecule radiates (fluorescence), the frequency is lower than that of the exciting radiation as seen in Figure 3.

The emission rates (frequencies) of fluorescence are typically on the order of 10^8 s^{-1}, so that a typical fluorescence lifetime is near 10 ns [25]. This is a very rapid process compared to the phosphorescence lifetimes. The lifetime (τ) of a fluorophore, which is the average time between its excitation and its return to the ground state, will be described in Section 3.3.

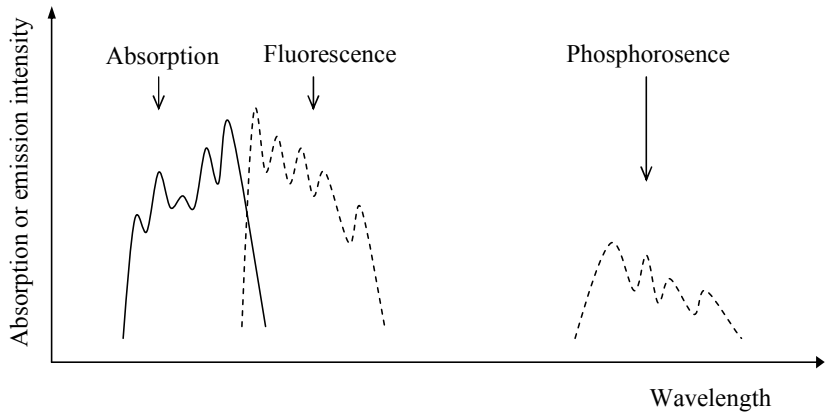

Fig.3. Schematic diagram showing absorption, fluorescence, and phosphorescence spectra [25].

3.1.3. Phosphorescence

Phosphorescence is the emission of light from triplet excited states. The ground state of a typical phosphorescent molecule is a singlet like its excited state. The different feature of a phosphorescent molecule, however, is that it possesses an excited triplet state. Ground state molecules absorb photons and go to excited singlet states as shown in Figure 1. After most of the excited molecules immediately fall down to the ground state, remaining molecules switch from the singlet state to the triplet state by spin-orbit coupling, the step which was called as intersystem crossing. The molecules in the triplet state lose some of their energy due to the mentioned non-radiative processes and finally they arrive to the bottom of the state [26].

As the transition from T_1 to the singlet ground state is forbidden, the emission rates are fairly slow, typically 10^3 to 1 s^{-1}, so that the phosphorescence lifetimes are on the order of milliseconds to seconds [25]. It is forbidden for a triplet state to convert into a singlet state because the spin of one electron cannot reverse in direction relative to the other electron during a transition. However, it is not totally prohibited because the spin-orbit coupling responsible for the intersystem crossing also breaks this rule.

Phosphorescence occurs at longer wavelengths (lower energy) relative to the fluorescence (see Fig.3).

The comparison between the lifetimes of fluorescence and phosphorescence is shown in Figure 4. In fluorescence, the spontaneously emitted radiation ceases immediately after the excitation. While in phosphorescence, the spontaneous emission may persist for long periods.

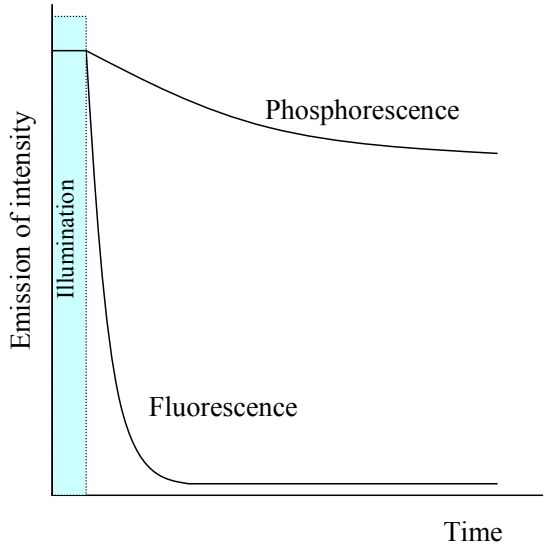

Fig.4. Fluorescence lifetime decays immediately after excitation. Phosphorescence continues with slowly diminishing intensity [26].

3.2. Introduction to Fluorescence Lifetimes

The phenomenon of molecular fluorescence emission contains both spectral and time information. Thus, fluorescence measurements can be classified into two types of measurements, steady-state and time-resolved [24]. Steady-state measurements are performed with constant illumination and observation. The sample is illuminated with a continuous beam of light, and the intensity or emission spectrum is recorded. The resultant spectrum is a well-known graph of intensity versus frequency or wavelength.

On the other hand time-resolved measurements are used for measuring intensity decays. The sample is exposed to a pulse of light, where the pulse width is typically shorter than the decay time of the sample. The intensity decay is recorded with a high-speed detection system that permits the intensity to be measured on the time scale [24]. In time-resolved measurements, there are two types of methods for measuring fluorescence lifetimes. One is pulse fluorometry, which relates to measurements

performed in the time domain, and the other is phase and modulation fluorometry, relating to the frequency domain [28]. Figure 5 shows the pulse fluorometry technique.

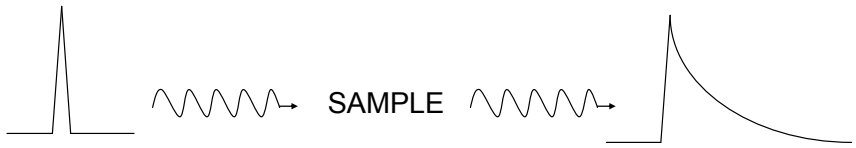

Pulsed source

Fluorescence response

$$i_F(t) = \frac{1}{\tau} e^{-t/\tau}$$

τ = Fluorescence lifetime

Fig.5. Principles of pulse technique for measuring fluorescence lifetimes [28].

The fluorescence lifetime or decay time of a molecule can be defined in the time-domain in terms of the rate of depopulation of the first excited singlet state (S_1) following a δ-function optical excitation from the ground state (S_0). Denoting the level population of the excited state to be N_2, we can employ the following rate equation from Chapter 2 to give the exponential decay

$$\frac{dN_2}{dt} = -\frac{N_2}{\tau_r}$$

which gives a fluorescence response function of the form

$$N_2(t) = N_2(0)\exp(-t/\tau_r),$$

where $N_2(0)$ is the initial number of atoms in the excited state and τ_r is the molecular fluorescence lifetime [23].

Because the excited state population is proportional to the fluorescence quantum intensity, the fluorescence lifetime can be determined experimentally by measuring the time taken for the fluorescence intensity to fall to $1/e$ of its initial value following the δ-function excitation. This is the basis of the time-correlated single-photon counting technique whereby the quantum nature of light enables the time distribution of individual photons within the decay profile to be recorded [28].

The dependence of τ on the rates of decay pathways is:

$$\tau_r = 1/(k_r + k_{nr}) = 1/k$$

where k_r is the radiative rate parameter, k_{nr} is the non-radiative rate parameter, and k the total decay rate (all have units in s^{-1}).

The radiative rate parameter k_r and the purely radiative lifetime τ_r are described in quantum mechanical terms by the Einstein A_{21} coefficient, of which there is detailed information in Chapter 2. The lifetime of the fluorophore in the absence of non-radiative processes is given as

$$A_{21} = k_r = 1/\tau_r$$

The meaning of the lifetime is best represented by a simplified Jablonski diagram shown in Figure 6.

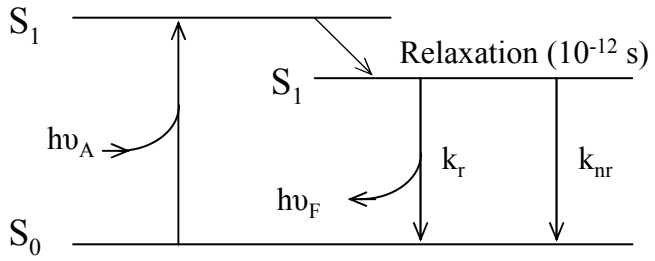

Fig.6. Jablonski diagram showing radiative and non-radiative rate parameters [24].

3.3. Time-Domain Lifetime Measurements

Time-domain (pulse fluorometry) lifetime measurements were performed in our experiments. Thus the frequency-domain methods will not be explained throughout this thesis. As it is mentioned before, in time-domain or pulse fluorometry, the sample is excited with a pulse of light (see Figure 5). The width of the pulse is made as short as possible and is preferably much shorter than the decay time τ of the sample. The time-dependent intensity is measured following the excitation pulse, and the decay time τ is calculated from the slope of a plot of *log I(t)* versus *t*, or from the time at which the intensity decreases to 1/*e* of the value at *t=0* [24].

3.3.1. Time-Correlated Single Photon Counting

Time Correlated Single Photon Counting (TCSPC) has been one of the best ways of measuring fluorescence decay times [29]. Today almost all time-domain measurements employ TCSPC. The principles of TCSPC can be understood from the instrument schematic shown in Figure 7. The experiment starts with the excitation pulse, which excites the sample and starts the time measurement clock.

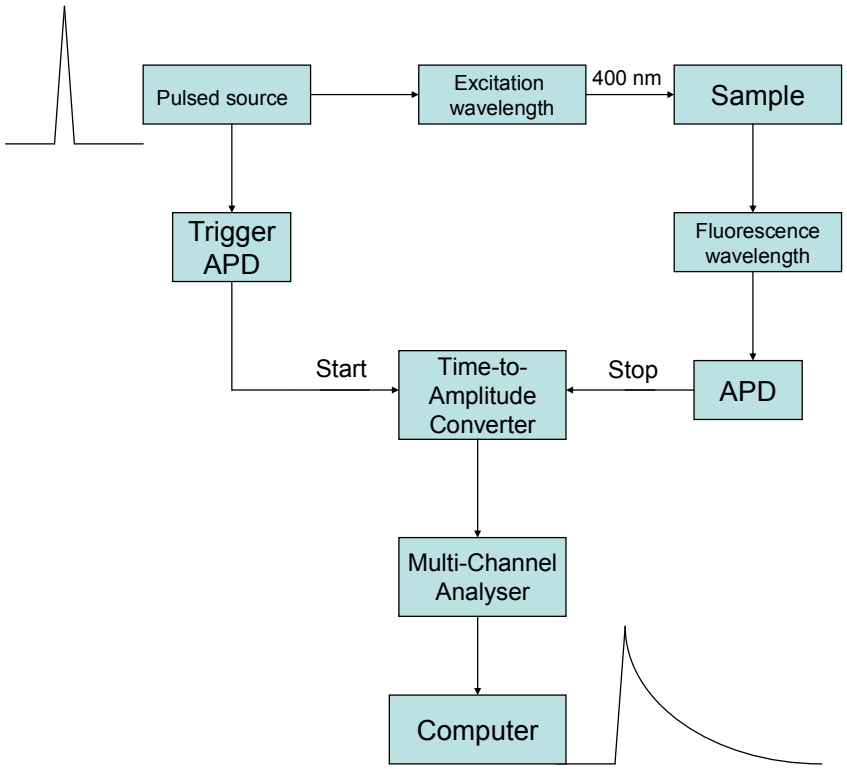

Fig. 7. Schematic for Time-Correlated Single Photon Counting

TCSPC is a digital technique, counting photons which are time-correlated in relation to the excitation pulse. Time-to-amplitude converter (TAC), which can be considered to be analogous to a fast stopwatch, is at the heart of this method.

The sample is repetitively excited using Femtosecond Ti:Sa laser. Each pulse is optically monitored by an avalanche photodiode to produce a start signal which is used to trigger the voltage ramp of the TAC. The voltage ramp is stopped only when the first fluorescence photon from the sample hits the other avalanche photodiode. The TAC provides an output pulse whose voltage is proportional to the time between the start and stop signals, that is the TAC correlates the start and stop signal. A computer-controlled multichannel analyzer (MCA) converts this voltage to a time channel using an analog-to-digital converter. Summing over many pulses, the MCA builds up a probability histogram of counts versus time channels [24]. The experiment is continued until enough counts in the peak channel are collected.

CHAPTER 4

EXPERIMENTAL

Under the guidance of the Purcell effect [7], which is explained in Chapter 2, we have aimed to modify the spontaneous emission rate of perylene dye molecules by embedding them into different polymer matrices with varying geometries. Sample preparations on one side and time-domain fluorescence lifetime measurements on the other side have formed the two complementary parts of the experiments.

This chapter describes the properties of perylene molecules and the preparation techniques of the perylene embedded polyacrylonitrile (PAN) nanofibers and polymethylmethacrylate (PMMA) films. The optical experiments performed to measure the fluorescence spectroscopy and lifetimes will also be explained in detail.

4.1. Perylene as a Fluorophore

Fluorescence typically occurs from aromatic molecules. One widely encountered fluorescent substance (fluorophore) is a polynuclear aromatic hydrocarbon, perylene, which was used as the emitting molecule in all our experiments. The chemical structure of the organic perylene compound is shown in Figure 1.

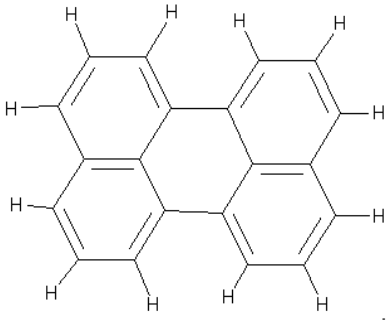

Fig.1. Chemical structure of perylene, $C_{20}H_{12}$ [30].

Perylene present in a solvent such as cyclohexane, benzene, or toluene is generally excited by violet and near-UV light. Upon return to the ground state, the perylene emits yellow and orange light with a wavelength around 480 nm. Absorption and fluorescence emission spectra of perylene are shown in Figure 2. Emission spectra vary widely and are dependent upon the chemical structure of the fluorophore and the solvent in which it is dissolved.

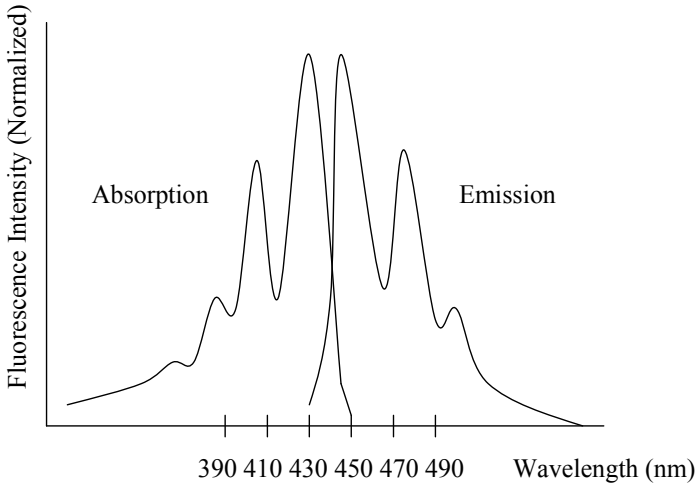

Fig.2. Absorption and fluorescence spectra of perylene dissolved in benzene [24].

We have obtained perylene dye molecules from Fluka Co. and used them as received. They were dissolved in pure toluene with a 10^{-3} molar concentration. The sample was then prepared after evaporating the toluene on a glass sample holder.

The fluorescence spectroscopy setup, that is shown in Figure 3, uses the second harmonic output (400 nm) of a mode-locked Ti:Sa laser (Coherent Mira 900-F) as the excitation source. The repetition rate of the laser is 76 MHz, thus producing pulses every other 13 ns. The excitation beam is focused onto the sample to a diffraction-limited spot using a microscope objective of 0.55 numerical aperture with a working distance of 10.1 mm (Nikon ELWD 50x). To separate the fluorescence emission from the excitation, suitable dichroic mirrors, emission and excitation filters are used. The emission of perylene is detected from the front side of the film using confocal fluorescence microscopy, which employs the same lens both for excitation and collection of the induced emission of the dye molecules. These fluorescence photons collected by the same objective are subsequently focused on a S2000 fiber optic spectrometer (Ocean Optics).

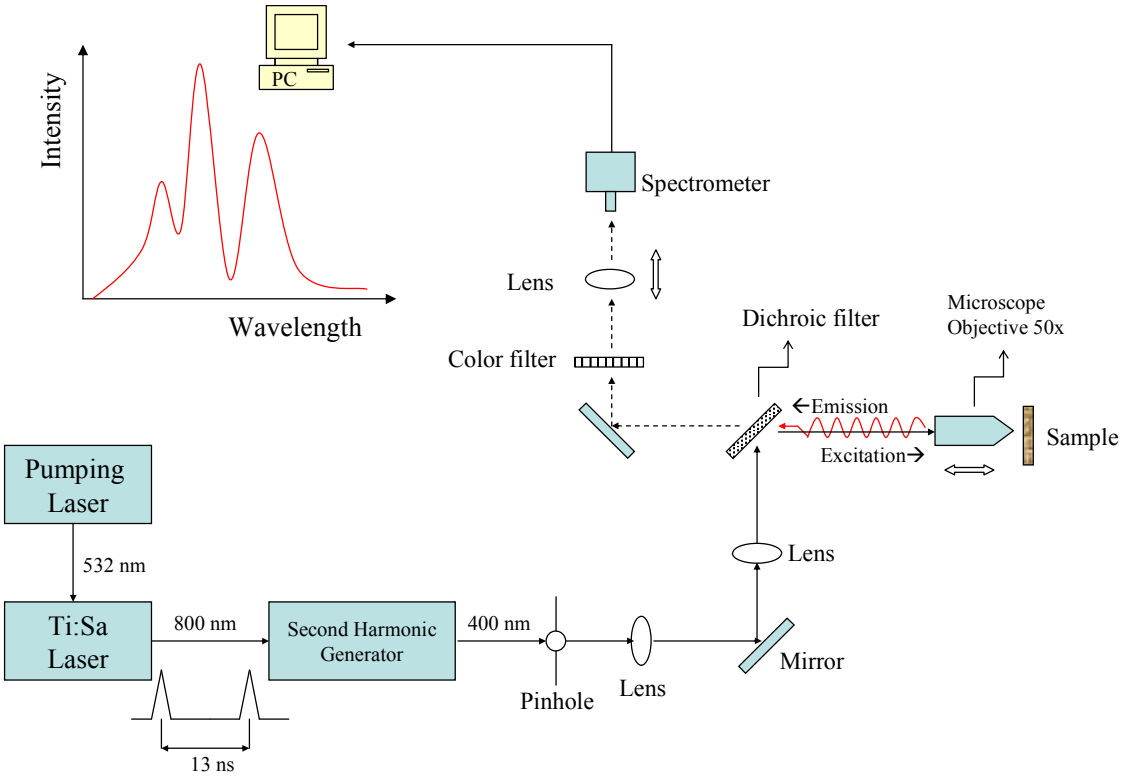

Fig.3. The schematic of the fluorescence spectroscopy setup.

Fluorescence lifetime is one of the most important characteristics of a fluorophore, as it determines the time available for the fluorophore to interact with or diffuse in its environment [24]. Several fluorescence lifetimes of perylene dissolved in different solvents were reported in the literature. For example, a perylene lifetime was found to be 4.6 ns in glycerol [20], 4.5 ns in cyclohexane [21], and between 3.9 and 6.2 ns in toluene with different concentrations [22]. In addition, perylene lifetimes of 6.31 ns was reported [31] when perylene is in DPPC bilayers in the gel phase, between 5.7 and 7.13 ns was reported [32] when perylene is in human erythrocyte ghosts, and between 9 and 11 ns was reported [33] when different polyvinyl alcohol (PVA) concentrations were added to a water suspension of perylene.

The fluorescence lifetime of perylene, as a result, can change drastically depending on the solvent it is being solved and the environment it is in. The meaning of the fluorescence lifetime is explained in Section 3.2, and the methods for measuring the lifetime is presented in Section 3.3.

In addition to the fluorescence lifetime, quantum yield of a fluorophore is also very important. The quantum yield is the number of emitted photons relative to the number of absorbed photons [24].

$Q = \frac{\Gamma}{\Gamma + k_{nr}}$ where Γ is the emission rate and k_{nr} is the rate of nonradiative decay to S_0.

One of the reasons why perylene was chosen as a fluorophore in our experiments is that it has a large quantum yield, that is $k_{nr} << \Gamma$, and it displays a very bright emission.

4.2. Lifetime Measurements

The decay times of the excited states were measured using single photon counting techniques. The spontaneous emission rate, the radiative decay lifetime in other words, of the pure perylene samples were measured by setting up a time-correlated single photon counting (TCSPC) experiment which was explained briefly in Chapter 3. The experimental schematic of the TCSPC is very similar to that of the spectroscopy setup shown in Figure 3. The only difference is that photon counting modules (avalanche photodiodes) replace the spectrometer and time correlating electronics follow the photodiodes. The detailed schematic of the experiment is shown in Figure 4.

The emission from the sample is collected by the same microscope objective, which focuses the excitation pulses onto the sample surface. This convenient way of collecting the emission is known as confocal microscopy, as mentioned in Section 4.1, and is very crucial in doing such kind of lifetime experiments, in which any possible loss in the emission light is undesirable. In confocal microscopy the excitation light is focused to a diffraction limited spot. Its size depends on the excitation wavelength and the numerical aperture (NA) of the objective used. The radius of the spot is approximately equal to $\lambda_{excitation}/4$, which corresponds to 100 nm in our case.

The second most critical equipment in this microscopy setup is the dichroic filter (or mirror), which is mounted at a 45° angle with respect to the excitation light and selectively permits the emission wavelength and forbids the unwanted excitation wavelength components that are reflected backwards from the sample surface. Our dichroic filter is designed to reflect light below 410 nm; thus, our excitation wavelength of 400 nm is reflected by the dichroic mirror, while the emission wavelengths (see Figure 2) are all transmitted.

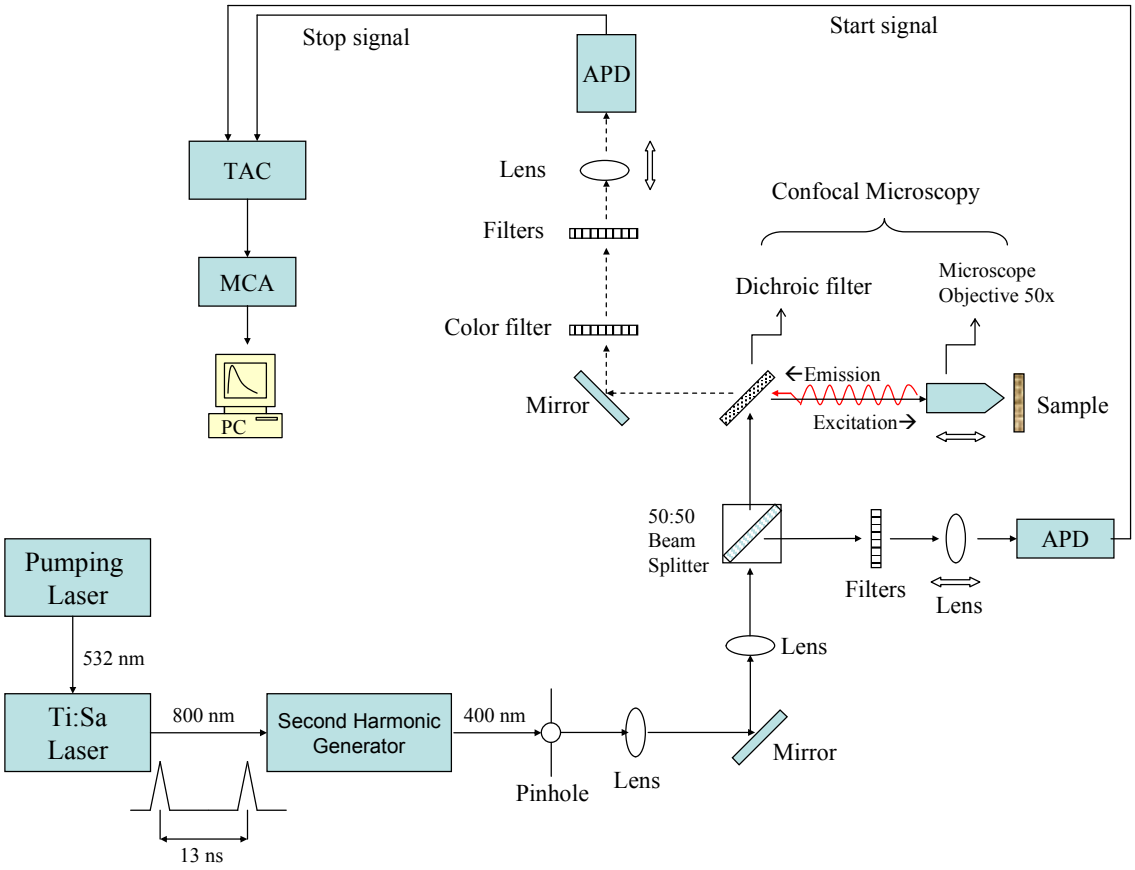

Fig.4. The schematic of the time-domain lifetime measurement setup.

The reference signal and the emission signal are collected by two different avalanche photodiodes (APDs, SPCM-AQR-14, Perkin Elmer) and are sent to the time-to-amplitude converter (TAC) in order to be correlated. The correlated output signal from the TAC is then transmitted to multi-channel analyzer (MCA) and then to the computer and the decay lifetime of the fluorescing sample (i.e., perylene) is measured. Detailed explanations of the optical instruments used in the experiments will be given in Section 4.4.

4.3. Polymers as Host Media for Perylene

As host matrices we chose polyacrylonitrile (PAN, $(C_3H_3N)_n$, 85000 g/mol) and polymethylmethacrylate (PMMA, $(C_5O_2H_8)_n$, 15000 g/mol) polymers. The chemical structures of the polymers are presented in Fig.5.

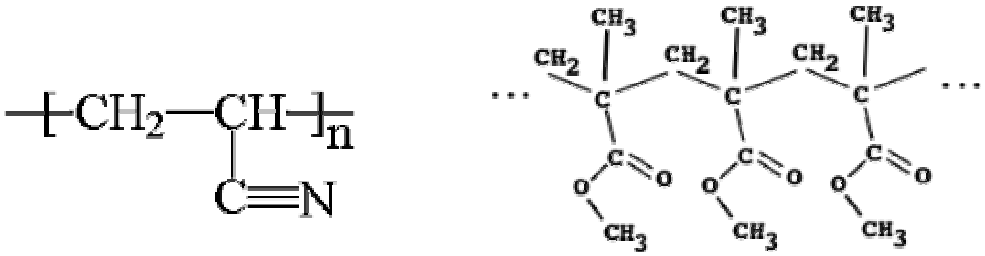

Fig.5. Chemical structures of PAN on the left and PMMA on the right.

4.3.1. Electrospun Polyacrylonitrile (PAN) Nanofibers

Electrospinning, or the former name electrostatic spinning, is a very good technique for the fabrication of polymer nanofibers. A schematic diagram to interpret electrospinning of polymer nanofibers is shown in Figure 7. A high voltage supplier, a capillary tube with a pipette or needle of small diameter, and a metal collecting screen are the three basic components used in the process. A high voltage, in the range of 20 kVs, is used to create an electrically charged jet of polymer solution or melt out of the pipette. Before reaching the collecting screen, the solution jet evaporates or solidifies, and is collected as an interconnected web of small fibers [34].

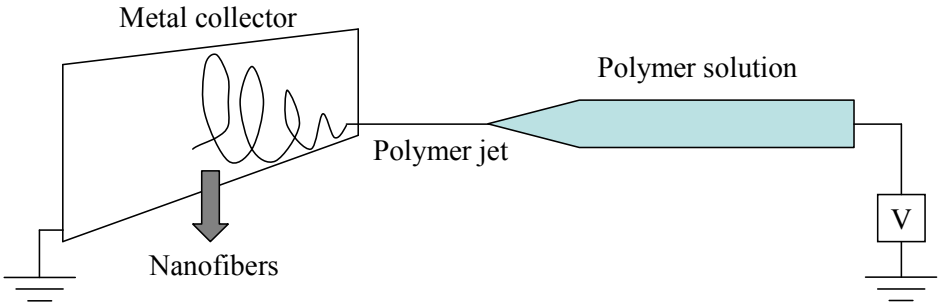

Fig.6. Polymer nanofibers formed by electrospinning.

Polyacrylonitrile (PAN) with a number average molecular weight of 85.000 g/mol was first dissolved in DMF, and only the 3.7 % of the solution consisted of PAN. Then 0.002 g of perylene was added to the 2 g of the PAN solution. The perylene in the blend was dissolved completely after adding 0.4 g of tetrahydrofuran (THF). After vigorous stirring, a pale yellow blend was formed. The polymer fluid is then introduced into the capillary tube for electrospinning. Both the dissolution and the electrospinning are essentially conducted at room temperature under atmospheric conditions. Very high DC voltage (in the range of 20 kVs) was applied, and the electrospinning was realized.

Many parameters can influence the transformation of polymer solutions into nanofibers through electrospinning. These parameters include (a) the solution properties such as viscosity, elasticity, conductivity, and surface tension, (b) governing variables such as hydrostatic pressure in the capillary tube, electric potential at the capillary tip, and the gap (distance between the tip and the collecting screen), and (c) ambient parameters such as solution temperature, humidity, and air velocity in the electrospinning chamber [34]. It is by no means an easy task to control the diameters of the fibers, which intrigues us. As a result, the fiber diameters are seldom uniform. Another generally encountered problem in the electrospinning is that defects such as beads may occur among polymer nanofibers, which badly affects the homogeneity of the sample.

4.3.2. Polymethylmethacrylate Films

The blend of polymethylmethacrylate (PMMA) and perylene molecules with a molarity of 10^{-3} M was dissolved completely in a pure toluene solution for two hours. The concentration of the dyes in the resulting films was kept low in order to ensure the confinement. The number average molecular weight of PMMA was 15000 g/mol. The solution was then coated onto cleaned glass cover slides and a few μm-thick films were prepared. The samples were dried either under air or under Nitrogen gas flow. Perylene molecules were expected to get confined in the PMMA matrices, and a modification of the emission rate was aimed.

4.4. Instrumentation for Time-Correlated Single Photon Counting

As the typical fluorescence lifetimes of many fluorophores are on the order of nanoseconds level, measurement of the time-resolved emission requires sophisticated optics and electronics in order to sense such short timescales. The features of the instruments that are used in our experiments are explained in this section.

4.4.1 Femtosecond Titanium:Sapphire Laser

Titanium-sapphire lasers emit near-infrared light, tunable in the range from 650 to 1100 nanometers. They are mainly used in time-correlated single photon counting experiments because of their possibility of generating ultrashort pulses. Titanium-sapphire refers to the lasing medium, a crystal of sapphire (Al_2O_3) that is doped with titanium ions. A Ti:sapphire laser is usually pumped with another laser with a wavelength of 514 to 532 nm (green light), for which Argon lasers (514.5 nm) and frequency-doubled Nd:YAG, Nd:YLF, and Nd:YVO_4 (527-532 nm) are used. Ti:sapphire lasers operate most effectively at a wavelength of 800 nm. In our laboratory, we have used a Coherent Mira 900-F Ti:sapphire laser, which is pumped with a diode-pumped solid-state Nd:YVO_4 laser (Coherent Verdi). The Nd:YVO_4 laser gives a maximum 20 Watts of continuous wave at 532 nm. Typically Ti:sapphire lasers are pumped with a power of 5 or 10 Watts. Although the long-wavelength output, from 650 to 1100 nm, of Ti:sapphire lasers is considered to be a disadvantage, we have generated 400 nm pulses after frequency doubling the Ti:sapphire output of 800 nm. 400 nm as an excitation wavelength is perfectly absorbed by perylene molecules. After the 76-MHz pulses exit the laser, the desired pulses can also be selected with a pulse picker to decrease the repetition rate.

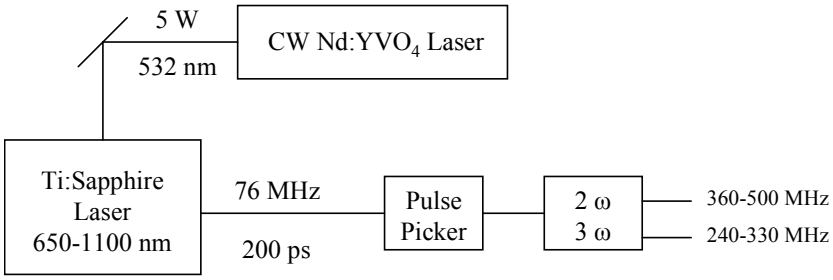

Fig.7. Femtosecond Ti:sapphire laser [24].

4.4.2. Avalanche Photodiode as a Detector

Avalanche photodiodes (APDs) have adequate gain and can be as fast as photomultiplier tubes (PMTs). The main problem is the small active area. In a PMT the area of the photocathode is typically 1cm x 1cm and is frequently larger. Photons arriving anywhere of the photocathode are detected. On the other hand, the active area

of an APD is usually less than 1 mm^2. It is 0.025 mm^2 in our high speed AQR-14 APDs (Perkin Elmer), which have a dark count of maximum 100 photons per second and a maximum light count of around 10 million photons per second measured by a Ratemeter (Ortec 661). It is therefore very difficult to focus the fluorescence onto the APDs [24]. APDs have been successfully used in TCSPC, and values of the fwhm from 20 to 400 ps have been reported [35-38].

4.4.3. Time-to-Amplitude Converter (TAC)

The role of the TAC, as mentioned in Section 3.4.1, is to measure the time between the excitation pulse and the first arriving emitted photon, which are the start and stop pulses, respectively. This is accomplished by charging a capacitor during the time interval between the pulses. Typically, the capacitor is charged from 0 to 10 V [24]. The time range available in the TAC we have (Ortec 567) starts from 50 ns and goes up to 2 ms. If the chosen range is 50 ns, for instance, the capacitor is fully charged at 50 ns. If a stop pulse is received at 25 ns, the charging is stopped at 5 V. If a stop pulse is not received, then the TAC is reset to zero. The linearity of the TAC is very important. If the voltage is not linear with time, then the data will contain systematic errors.

4.4.4. Multichannel Analyzer (MCA)

The MCA, which is an interfacing card between the TAC and computer, measures the voltage pulses from the TAC and sorts them according to counts at each particular voltage (time) [24]. The MCA first performs an analog-to-digital conversion. The histogram of the number of counts at each voltage (time) is displayed on the computer. This histogram represents the measured intensity decay. The MCA we used has 2048 channels.

CHAPTER 5

RESULTS AND DISCUSSION

Before embedding perylene molecules into polymer matrices, it is necessary to investigate the optical properties of perylene and to measure its decay lifetime, as it will be considered as a reference when comparing the modified lifetimes.

5.1. Perylene Spectrum

Figure 1 shows the emission spectrum of the perylene, which was recorded using the experimental setup described in Section 4.1. The excitation wavelength was 400 nm. It is shown that there are three emission peaks in the spectra which are located at 450, 480, and 510 nm, as stated in the literature [22,31,39].

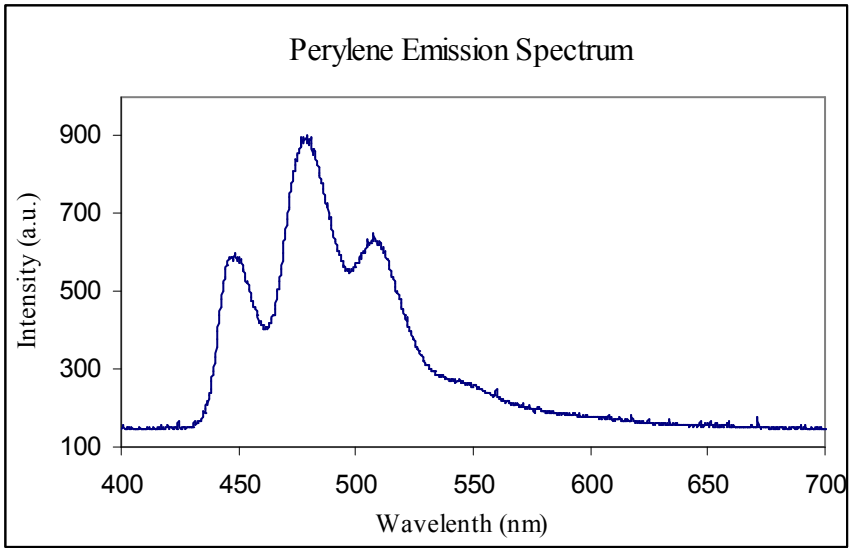

Fig.1. Emission spectrum of perylene dissolved in toluene.
Excitation wavelength is 400 nm.
Three emission peaks are located at 450 nm, 480 nm, and 510 nm.

5.2. Perylene Lifetime Measurements

The prepared perylene samples were scanned over the focus of the excitation spot. Once the fluorescence was observed, it was focused onto the avalanche photodiode (APD) and several lifetime data were obtained from different parts of the samples.

The fluorescence lifetime is determined using time-correlated single photon counting [40] by plotting a histogram of time lags between the excitation pulses and the detected fluorescence photons, as also described in Section 3.3. The exponential fit to the observed decay profile gives the fluorescence lifetime. The experimental setup of lifetime measurements is shown in Section 4.2.

Three different lifetime data obtained from perylene are plotted in Figure 2. The data are obtained from different parts of the sample. They all give a consistent lifetime of perylene, which is about τ = 4.8 ns. This decay time is calculated from the time at which the intensity decreases to 1/*e* of the value at t=0.

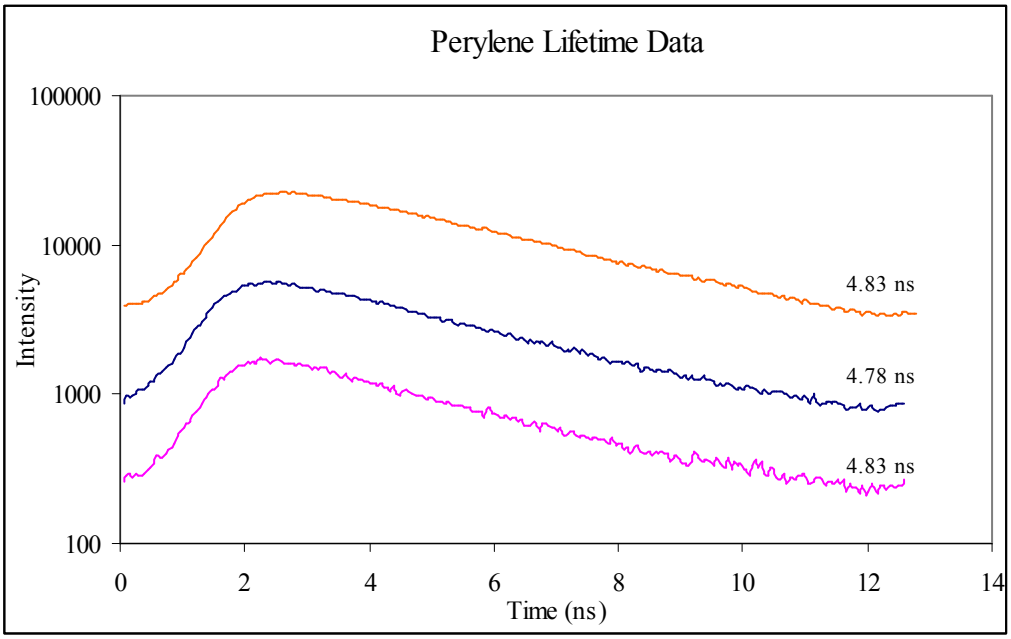

Fig.2. Decay lifetime of perylene, which was found around 4.8 ns.

The best fit lines (trendline, or also called the least-squares fit) of the decay curves and the equations of these trendlines are shown in Figure 3. The second decay curve in the figure, for instance, has a trendline with the equation $y = 5259\exp(-0.2091x)$, which helps us to easily calculate the lifetime from the exponential function.

The exponential functions of the trendlines have the form $e^{-\left(\frac{1}{\tau}\right)t}$. In the above case, the lifetime (4.78 ns) is found by inversing 0.2091.

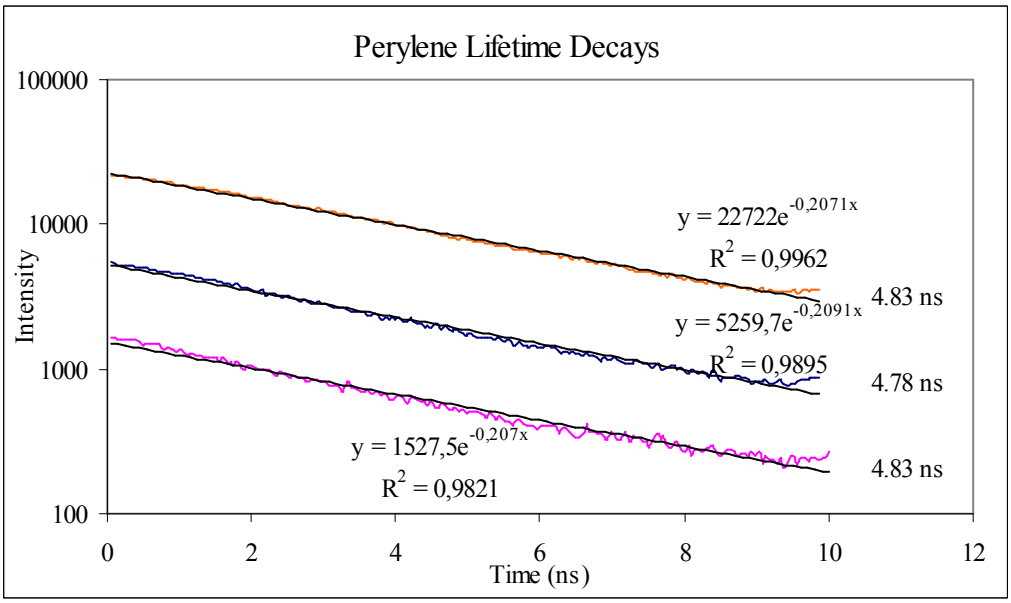

Fig.3. Decay lifetime curves of perylene with trendlines on them.

The R^2 values of the trendlines give the relationship between two variables, which is found to be above 0.98 in all the decay curves in Figure 3. This value ranges between 0 and +1, with complete correlation expressed as +1. The greater the R^2 value, the better the fit of the line to the actual data. As it is seen, the R^2 values of the above trendlines are almost 1, which means that the lifetime calculated from the trendline equations are very reasonable. The lifetime decays become much smoother and the R^2 values increase as the number of collected counts (intensity) increase. As we collect more counts, the correlation between the trendline and the actual data increases, thus producing better results.

Having learned the fluorescence decay lifetime of perylene, we then prepared some polymer/perylene blends and embedded perylene molecules into polymer matrices in order to measure any possible modification in the spontaneous emission rate, thus the radiative lifetime of the molecules.

5.3. Electrospun Polyacrylonitrile Nanofibers as a Host Media for Perylene

Perylene embedded nanofibers of polyacrylonitrile (PAN) have been prepared using the electrospinning process explained in Section 4.3. Before going into the measured spontaneous emission (fluorescence) lifetimes of these samples, it is very important to analyze the structures and dimensions of these nanofibers. It is desirable to have nanofibers with dimensions smaller than 450 nm, as we know that the dimensions of the geometries have to be smaller than the emission wavelength of the fluorophore (perylene) in order the spontaneous emission to be inhibited. Nanofibers with diameters much smaller than 450 nm will always better serve our purpose of confining perylene molecules.

SEM photographs of the fabricated perylene embedded nanofibers with sizes of 158, 435, 441 and 747 nm are displayed in Figure 4.

As seen from the images, it is not possible to talk about uniformity in the diameters of nanofibers. The diameters range approximately from 150 nm to 800 nm, which have very different confinement affects on peryelene molecules. Compared to the emission wavelength of perylene (between 450-510 nm), a confinement of 150 nm is considered to be a pretty enough size for realizing inhibited spontaneous emission. It is known from Purcell [7] that spontaneous emission is inhibited if the cavity has characteristic dimensions which are small compared to the radiative wavelength. On the other hand, nanofibers with diameters comparable to our emission wavelength are not expected to inhibit the spontaneous emission rate as much as the nanofibers with 150 nm diameters.

Figure 5 shows SEM photographs of beads formed during the electrospinning process. Even though the beads are not desirable for our purposes, they do not have any affect on the inhibited spontaneous emission because of their very large sizes.

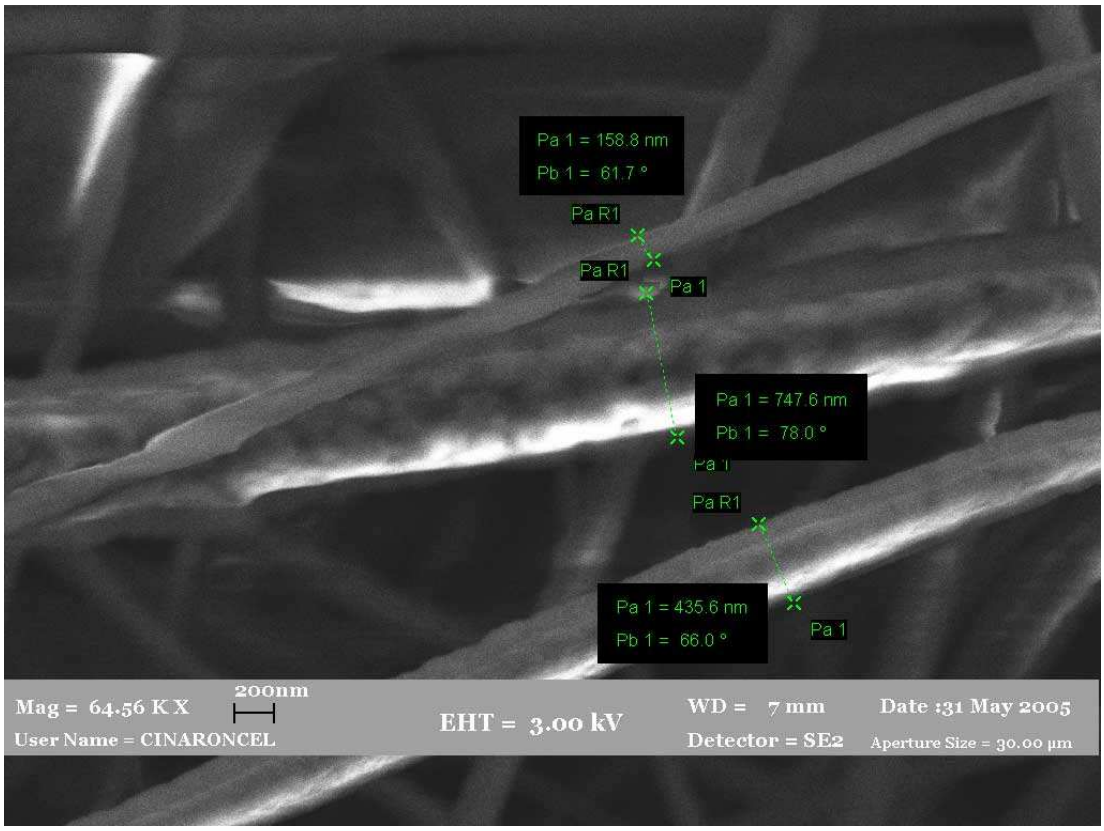

(a)

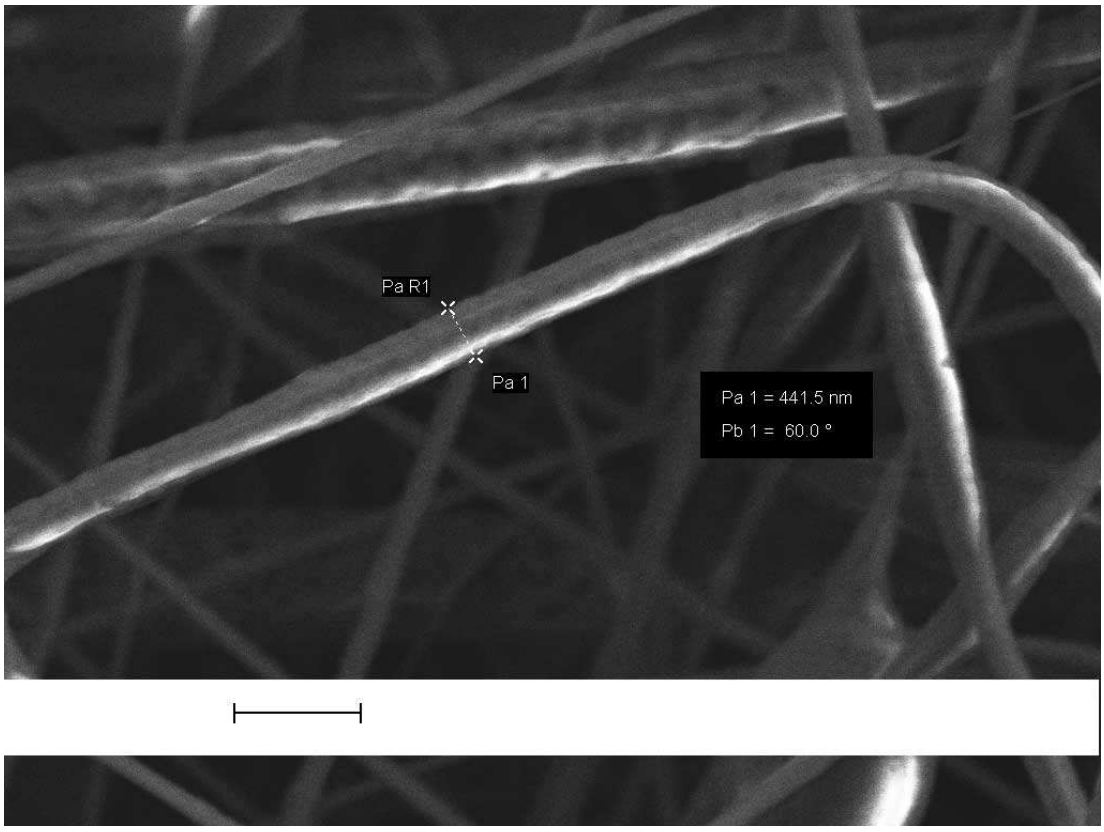

(b)

Fig.4. SEM photographs of perylene embedded PAN nanofibers of different diameters: (a) 158, 435, and 747 nm (b) 441 nm.

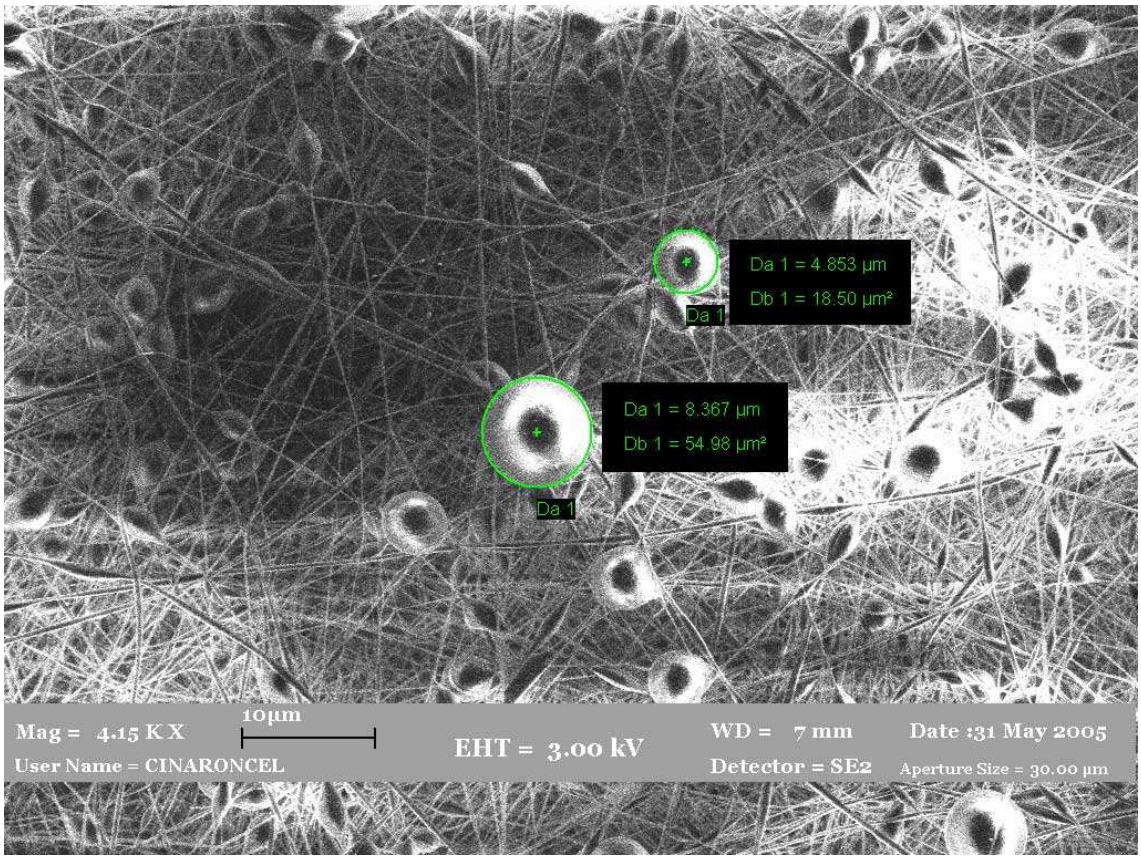

Fig.5. SEM photographs of perylene embedded PAN nanofibers. Beads of different sizes: 8.3 and 4.8 µm among nanofibers are seen.

With these different nanofiber diameters in mind, we have realized lifetime measurements of the perylene embedded PAN nanofibers in the same manner as described in Section 5.2., using the same optical setup. By spatially moving the sample and focusing the excitation beam on different points on the sample, we have obtained a distribution of lifetimes as shown in Figures 6 and 7.

The lifetime data shown these figures prove a gradual increase in the perylene lifetime due to the cavity effect, which is clearly an evidence of the inhibition of the spontaneous emission rate. Because we do not know where exactly the excitation beam is focused on the surface of the sample, we can not certainly decide which lifetime corresponds to which size of nanofibers. But it is in a way possible to estimate that the beam focus is on a nanofiber with a diameter much less than our emission wavelength of 450 nm, when we measured a lifetime around 12 ns or greater.

A very slight increase in the perylene lifetime is observed (near 1 ns) in the curves with lifetimes 5.73 and 5.93 ns. These lifetimes' data might be coming from nanofibers with greater diameters, for example from nanofibers of sizes around 500 nm, which is a diameter comparable to the radiative wavelength. On the other hand, the

curves with lifetimes of 8.6 and 12.36 ns are very well considered as a significant increase in the lifetime of the perylene (4.8 ns). 8.6 ns is as much as two times an increase in the lifetime of perylene, and 12.36 ns is as much as three times an increase in the lifetime of perylene. These lifetime extensions (or spontaneous emission rate inhibitons) might be coming from perylene embedded nanofibers with smaller diameters, which have the ability to confine perylene better than greater sized nanofibers.

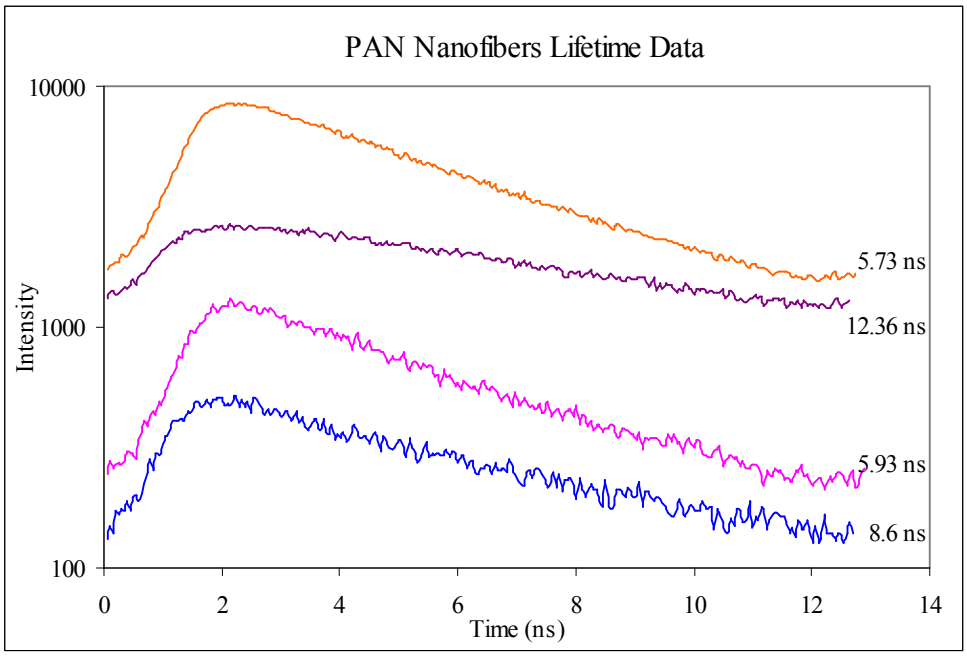

Fig.6. Perylene embedded PAN nanofibers' lifetimes.

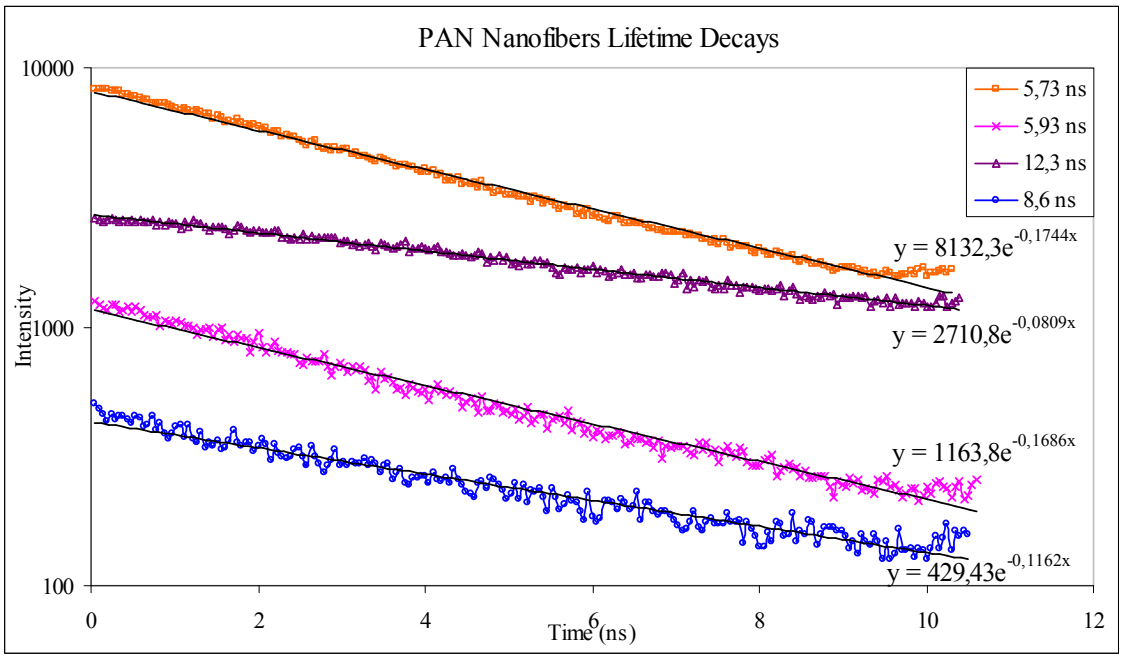

Fig.7. The decay lifetime curves with trendlines on them.

The lifetimes presented in Figure 7 were calculated by using the same method utilized in finding perylene lifetimes. The power of the exponential function gives the inverse of the lifetime τ. The R^2 values are very near to unity even though they were not included in the figure. The curve seen on the bottom of Figure 7 has an R^2 value of 0.95 and this value increases up to 0.991 for other curves as the intensity increases.

5.4. Polymethylmethacrylate Films as a Host Media for Perylene

Polymethylmethacrylate (PMMA)/perylene blend was prepared as stated in Section 4.3 and coated onto cleaned glass slides with an approximate thickness of a few μm. The films proved high absorption intensity at the excitation wavelength of 400 nm, which is necessary in our case. Figure 8 shows the absorption spectrum of perylene embedded PMMA films taken by a UV-VIS Shimadzu spectrometer.

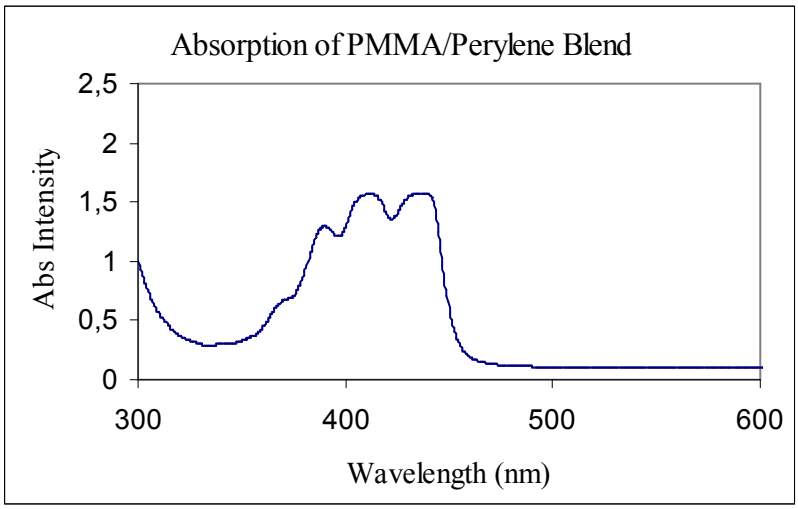

Fig.8. The absorption spectrum of perylene embedded in PMMA films.

By focusing the excitation beam on different parts of the film, the fluorescence lifetime data were measured using the same techniques as in the case of perylene and PAN nanofibers. Lifetime data are presented in Figures 9-12.

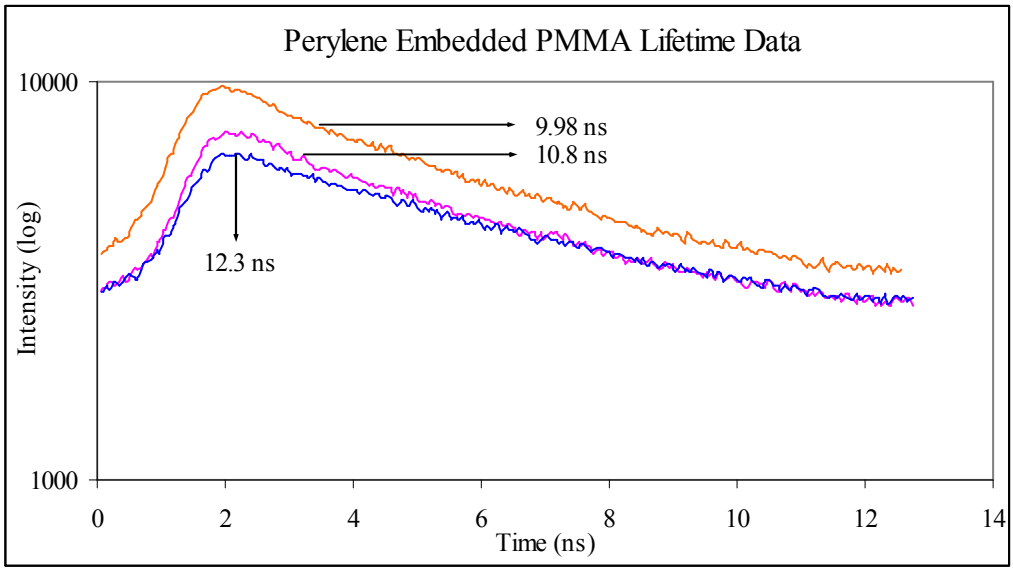

Fig.9. Perylene embedded PMMA films' lifetime data.

Confining perylene emission fields into PMMA dielectric structures modify the intrinsic polarizability of perylene [19]. Thus a significant modification of the lifetime of the excited molecular level, which is accompanied with a small shift of the corresponding occupied levels were observed. The data shown in Figure 9 is a very good evidence for inhibited emission rates of perylene.

The trendlines fit to the actual data and their equations are presented in Figures 10-12. As the R^2 values of the trendlines are very high, the calculated lifetimes are very reliable.

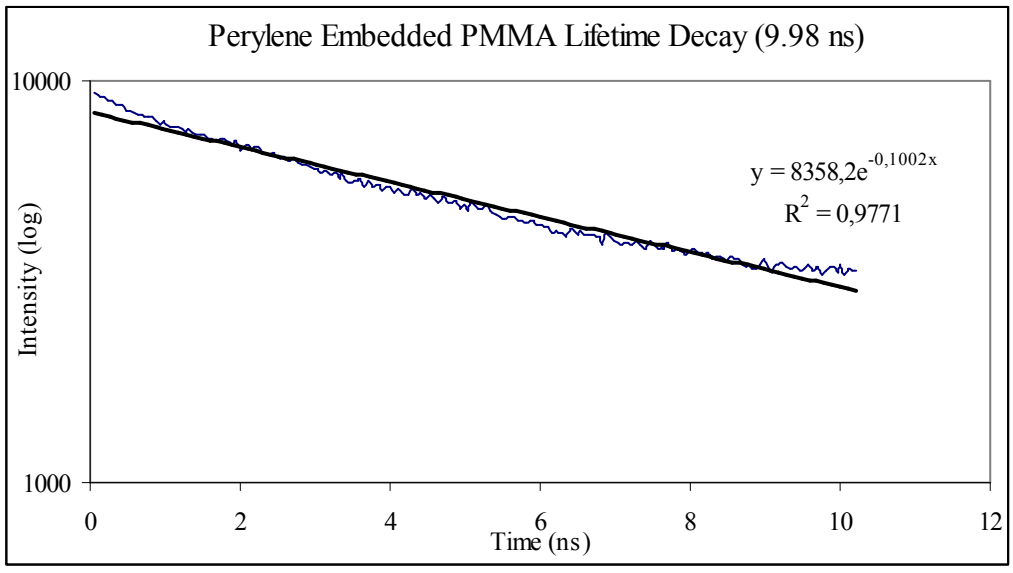

Fig.10. Perylene embedded PMMA film showing approximately 2 times an increase in the perylene lifetime.

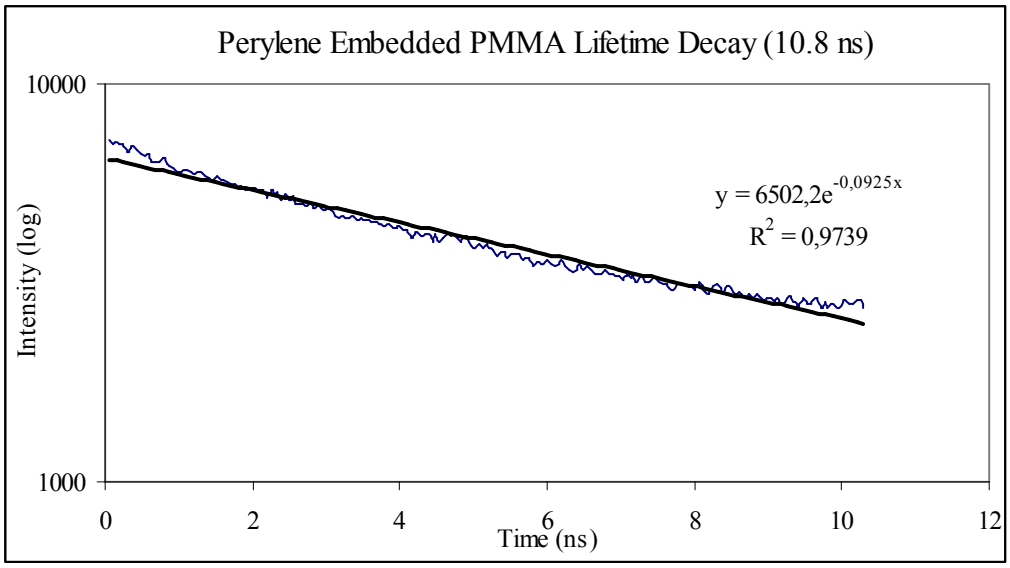

Fig.11. Perylene embedded PMMA film showing a greater increase in the lifetime.

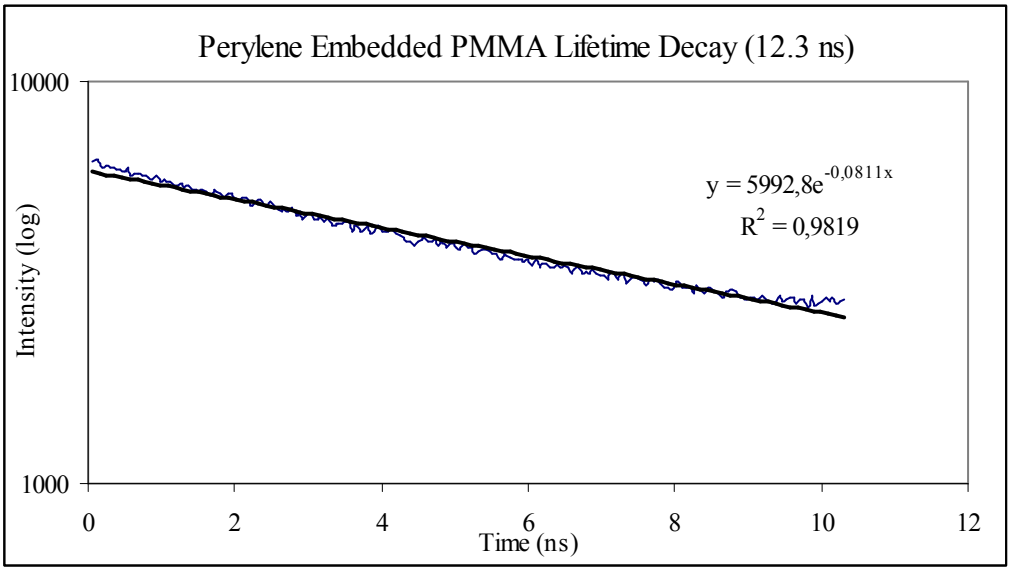

Fig.12. Perylene embedded PMMA film showing almost 3 times an increase in the perylene lifetime.

Although it is usually assumed that the decay rate of a molecule from its excited state is an intrinsic property of the molecule, Fermi's golden rule written in terms of the refractive index explicitly shows the dependence of the lifetime to the surrounding dielectric environment [12], the host medium.

$$\frac{1}{\tau_R} \propto \left(\frac{3}{\left(n_{\text{int}}^2 / n_{ext}^2 \right) + 2} \right)^2 \frac{n_{ext}}{n_{\text{int}}} \qquad (5.4.1.)$$

It is seen from this new version of Fermi's golden rule that simply changing the index of refraction of the surrounding medium can already have an effect on the spontaneous emission rates [12]. The spontaneous emission rate will depend on the refractive index n_{ext} of the host medium, which may be greater or less than the n_{int} of the radiating substance itself. Because perylene molecules behave like point sources, we can assign $n_{ext}= n_{air}=1$ and $n_{int}= n_{polymer}$, which is 1.5187 for PAN and 1.4893 for PMMA.

The lifetime formula given in equation (5.4.1) is generally used for thin films rather than small particles. The equation reduces to a simpler form when making approximations in two important limits: the film is either thinner or thicker than a half wavelength of radiation [12]. As our film thickness (few μm) is greater than half the emission wavelength (~ 250 nm), though still optically thin, the following relation applies in our case:

$$\frac{1}{\tau_R} \propto \frac{n_{ext}^2}{n_{\text{int}}^2} \qquad (5.4.2.)$$

Plugging the refractive index of the PMMA into the equation (5.4.2), we can find an approximate value for the lifetime to be 2.22 times the original perylene. Multiplying the declared perylene lifetime (4.8 ns) by 2.22, we can approximately find a value for the perylene doped PMMA films to be 10.65 ns. This calculated value is very near our experimentally measured values.

CHAPTER 6

CONCLUSION

Inhibited spontaneous emission of perylene dye molecules in subwavelength dielectric media has been demonstrated. The polymers polyacrylonitrile (PAN) and polymethylmethacrylate (PMMA) were used to change the fluorescence emission lifetime of perylene molecules, which was measured to be 4.8 ns. PAN and PMMA can confine the molecules of perylene, and the interactions between the polymers and the perylene molecules have some influence on the optical properties of perylene. The resulting spontaneous emission lifetimes were characterized by using time-correlated single photon counting.

Electrospun PAN nanofibers have been prepared and some interesting phenomena have been observed, such as enhancement of perylene lifetime with decreasing size of the nanofibers. As the dimension of nanofibers decreases, the decay time of the perylene excited states becomes longer owing to the shifts in the energy levels of the molecules due to modifications of the vacuum states. Decay lifetimes of perylene molecules are enhanced from 4.8 ns up to 12.36 ns for PAN nanofibers. PMMA films also exhibit an enhancement in the perylene decay lifetime, from 4.8 ns up to 12.3 ns, which results in almost 2.6 times an inhibition in the spontaneous emission rate.

As a future work, different polymers can be used as host media for different types of dye molecules, and lifetime measurements can be performed in order to observe a modification in the spontaneous emission rates. Higher refractive index polymers will be better candidates for observing inhibited spontaneous emission.

In addition, polarization dependent lifetime measurements can be studied as a future work, which will reveal the lifetime data of different polarized emitters entrapped in polymer matrices.

REFERENCES

1. Planck M., "On the Improvement of Wien's Equation for the Spectrum," *Verh. Dtsch. Phys. Ges.*, Vol. 2, pp. 202-204, 1900. "On the Theory of the Energy Distribution Law of the Normal Spectrum," *Verh. Dtsch. Phys. Ges.*, Vol. 2, pp. 237-245, 1900.

2. Einstein A., "On the Quantum Theory of Radiation," *Physikalische Zeitschreibung,* Vol. 18, pp. 121-128, 1917.

3. Haroche S. and Kleppner D., "Cavity Quantum Electrodynamics," *Physics Today*, pp. 24-30, Jan. 1989.

4. Schniepp H. and Sandoghar V., "Spontaneous Emission of Europium Ions Embedded in Dielectric Nanospheres," *Physical Review Letters*, Vol. 89, pp. 257403-1-4, 2002.

5. Kleppner D., "Inhibited Spontaneous Emission," *Physical Review Letters*, Vol. 47, No. 4, pp. 233-236, 1981.

6. Casimir H.B.G., and Poulder D., "The Influence of Retardation on the London-van der Waals Forces," *Physical Review*, Vol. 73, pp. 360-372, 1948.

7. Purcell E. M., "Spontaneous Emission Probabilities at Radio Frequencies," *Physical Review*, Vol. 69, pp. 681, 1946.

8. Drexhage K. H., "Influence of a Dielectric Interface o Fluorescence Decay Time," *Journal of Luminescence*, Vol. 1,2, pp. 693-701, 1970.

9. Hulet R.G., Hilfer E.S., and Kleppner D., “Inhibited Spontaneous Emission by a Rydberg Atom,” *Physical Review Letters*, Vol. 55, pp. 2137, 1985.

10. Jhe W., Anderson A., Hinds E.A., Meschede D., Moi L., and Haroche S., “Suppression of Spontaneous Decay at Optical Frequencies: Test of Vacuum Field Anisotropy in Confined Space,” *Physical Review Letters*, Vol. 58, pp. 666-669, 1987.

11. De Martini F., Innocenti G., Jacobovitz G.R., and Mataloni P., “Anomalous Spontaneous Emission Time in a Microscopic Optical Cavity,” *Physical Review Letters*, Vol. 59, pp. 2955, 1987.

12. Yablonovitch E., Gmitter T. J., and Bhat R., “Inhibited and Enhanced Spontaneous Emission from Optically Thin AlGaAs/GaAs Double Heterostructures,” *Physical Review Letters*, Vol. 61, pp. 2546-2549, 1988.

13. Heinzen D. J. , Childs J.J., Thomas J.F., and Feld M. S., “Enhanced and Inhibited Visible Spontaneous Emission by Atoms in a Confocal Resonator,” *Physical Review Letters*, Vol. 58, pp. 1320, 1987.

14. Lin H. B., Eversole J. D., Meritt C. D., and Campillo A. J., “Cavity-Modified Spontaneous Emission Rates in Liquid Microdroplets,” *Physical Review A*, Vol. 45, pp. 6756, 1992.

15. Chew H., “Radiation and lifetimes of atoms inside dielectric particles,” *Physical Review A*, Vol. 38, pp. 3410-3416, 1988.

16. Goy P., Raimond J.M., Gross M., and Haroche S., “Observation of Cavity-Enhanced Single-Atom Spontaneous Emission,” *Physical Review Letters*, Vol. 50, pp. 1903, 1983.

17. Berman P.R., “Cavity Quantum Electrodynamics,” San Diego: Academic, 1994.

18. Chang R.K., and Campillo A.J., "Optical Processes in Microcavities," Singapore: World Scientific, 1996.

19. Girard C., Martin O.J.F., and Dereux A., "Molecular Lifetime Changes by Nanometer Scale Optical Fields," *Physical Review Letters*, Vol. 75, pp. 3098-3101, 1995.

20. Barkley M.D., Kowalczyk A.A., and Brand L., "Fluorescence Decay Studies of Anisotropic Rotations of Small Molecules," *J. of Chemical Physics*, Vol. 75-7, pp. 3581-3593, 1981.

21. Johnson D.A., Nguyen B., Bohorquez A.F., Valenzuela C.F., "Paramagnetic Fluorescence Quenching in a Model Membrane: A Consideration of Lifetime and Temperature," *Biophysical Chem.*, Vol. 79, pp. 1-9, 1999.

22. Katoh R., Sinha S., Murata S., and Tachiya M., "Origin of the Stabilization Energy of Perylene Excimer as Studied by Fluorescence and Near-IR Transient Absorption Spectroscopy," *J. of Photochemistry and Photobiology A: Chem.*, Vol. 145, pp. 23-34, 2001.

23. Loudon R., "The Quantum Theory of Light, Third Edition," New York: Oxford University Press, 2003.

24. Lakowicz, J.R., "Principles of Fluorescence Spectroscopy, Second Edition," New York: Plenum Press, 1999.

25. Alberty R.A., and Silbey R. J., "Physical Chemistry, Second Edition," New York: Wiley, 1996.

26. Atkins P., "The Elements of Physical Chemistry, Third Edition," New York: Oxford University Press, 2001.

27. Jablonski A., "Über den Mechanisms des Photolumineszenz von Farbstoffphosphoren," *Z. Phys*, Vol. 94, pp. 38-46, 1935.

28. Lakowicz J.R., “Topics in Fluorescence Spectroscopy, Volume 1 Techniques,” New York: Plenum Press, 1991.

29. Bollinger L.M., and Thomas G.E., *Rev. Sci. Instrum*. Vol. 32, pp.1044 1961.

30. “Handbook of Fine Chemicals and Laboratory Equipment,” Berlin: Aldrich, 2003.

31. Birch D.J.S., Suhling K., Holmes A.S., Salthammer T., and Imhof R.E., “Metal Ion Quenching of Perylene Fluorescence in Lipid Bilayers,” *Pure and Applied Chem.*, Vol. 65, pp. 1687-1692, 1993.

32. Petrov E.P., Kruchenok J.V., and Rubinov A.N., “Effect of the External Refractive Index on Fluorescence Kinetics of Perylene in Human Erythrocyte Ghosts,” *J. of Fluorescence*, Vol. 9, pp. 111-121, 1999.

33. Xie R., Xiao D., Fu H., Ji X., Yang W., and Yao J., “Effect of PVA on the Growth and the Optical Properties of Perylene Nanocrystals,” *New J. of Chem.*, Vol. 25, pp. 1362-1364, 2001.

34. Huang Z-M., Zhang Y., Kotaki M., and Ramakrishna S., “A review on polymer nanofibers by electrospinning and their applications in nanocomposites,” *Composite Science and Technology*, Vol. 63, pp. 2223-2253, 2003.

35. Cova S., Ripamonti G., and Lacaita A., “Avalanche Semiconductor Detector for Single Optical Photons with a Time Resolution of 60 ps,” *Nucl. Instrum. Methods Phys.*, Vol. A253, pp. 482-487, 1987.

36. Lacaita A., Cova S., and Ghioni M., “Four-hundred Picosecond Single-Photon Timing with Commercially Available Avalanche Photodiodes,” *Rev. Sci. Instrum.*, Vol. 59, pp.1115-1121, 1988.

37. Cova S., Lacaita A., Ghioni M., Ripamonti G., and Louis T.A., "20-ps Timing Resolution with Single-Photon Avalanche Photodiodes," *Rev. Sci. Instrum.*, Vol. 60, pp.1104-1110, 1989.

38. Louis T.A., Ripamonti G., and Lacaita A., "Photoluminescence Lifetime Microscope Spectrometer Based on Time-Correlated Single-Photon Counting with an Avalanche Diode Detector," *Rev. Sci. Instrum.*, Vol. 61, pp.11-22, 1990.

39. Zhao J., Liu X., Wang L., Wang S., Liu Y., Ning Y., Wu D., Wu S., Jin C. Wang L., Jing X., and Wang F., "Stimulated Emission in the Film of Polymer/Dye Blend," *Thin Solid Films*, Vol. 363, pp. 201-203, 2000.

40. Tomczak N., Vall R.A.L., van Dijk E., Garc M., Kuipers L., van Hulst N.F., and Vancso D.J., "Probing Polymers with Single Fluorescent Molecules," *European Polymer Journal*, Vol. 40, pp. 1001–1011, 2004.